

000 001 002 003 004 005 SCHEDULERS FOR SCHEDULE-FREE: THEORETICALLY 006 INSPIRED HYPERPARAMETERS 007 008 009

010 **Anonymous authors**
 011 Paper under double-blind review
 012
 013
 014
 015
 016
 017
 018
 019
 020
 021
 022
 023

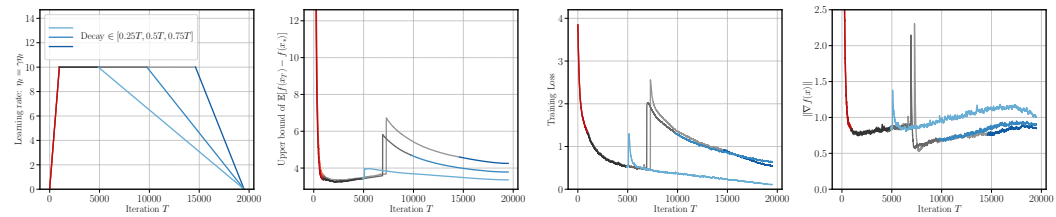
ABSTRACT

024
 025 The recently proposed **schedule-free** method has been shown to achieve strong
 026 performance when hyperparameter tuning is limited. The current theory for
 027 **schedule-free** only supports a constant learning rate, whereas the implemen-
 028 tation used in practice uses a warm-up schedule. We show how to extend the
 029 *last-iterate* convergence theory of **schedule-free** to allow for any scheduler,
 030 and how the averaging parameter has to be updated as a function of the learn-
 031 ing rate. We then perform experiments showing how our convergence theory has
 032 some predictive power with regards to practical executions on deep neural net-
 033 works, despite that this theory relies on assuming convexity. When applied to the
 034 warmup-stable-decay (**wsd**) schedule, our theory shows the optimal convergence
 035 rate of $\mathcal{O}(1/\sqrt{T})$. We then use convexity to design a new adaptive Polyak learning
 036 rate schedule for **schedule-free**. We prove an optimal *anytime* last-iterate con-
 037 vergence for our new Polyak schedule, and show that it performs well compared
 038 to a number of baselines on a black-box model distillation task.
 039
 040
 041

1 INTRODUCTION

042 The recently introduced *schedule-free* method (Defazio et al., 2024) achieves state-of-the-art perfor-
 043 mance over a range of deep learning problems, as proven by its winning entry for the MLCommons
 044 2024 AlgoPerf Algorithmic Efficiency Challenge Self-Tuning track¹.
 045

046 The efficacy of **schedule-free** on these highly non-convex deep learning problems is remarkable
 047 considered that it was designed for convex losses. Indeed, **schedule-free** achieves the optimal
 048 $\mathcal{O}(DG/\sqrt{T})$ convergence rate on the class of convex G -Lipschitz losses, for $D := \|x_0 - x_\star\|$,
 049 where x_0 and x_\star are the first and optimal parameters, respectively.
 050



051 Figure 1: Our theory (Theorem 2.1) is good at predicting the behavior of the training loss: The
 052 plots show the theoretical bound and the training loss of ResNet-20/Cifar10 when using **wsd**
 053 schedules with base learning rate $\gamma = 10$ and three different cooldown lengths. The gradient norm
 054 over the iteration is shown on the rightmost figure for reference. The red color denotes the warmup
 055 period, the gray color denotes the constant period, and the blue color denotes the cooldown period.
 056

057 We first extend the theory of **schedule-free** to allow for any learning rate scheduler. This is
 058 important because the current theory for **schedule-free** in (Defazio et al., 2024) only supports
 059 constant learning schedules, whereas in practice **schedule-free** method is applied with a warmup
 060 schedule. Although Defazio et al. (2024) has a bound that holds for arbitrary schedules (see Theorem
 061

062
 063
 064
 065
 066
 067
 068
 069
 070
 071
 072
 073
 074
 075
 076
 077
 078
 079
 080
 081
 082
 083
 084
 085
 086
 087
 088
 089
 090
 091
 092
 093
 094
 095
 096
 097
 098
 099
 100
 101
 102
 103
 104
 105
 106
 107
 108
 109
 110
 111
 112
 113
 114
 115
 116
 117
 118
 119
 120
 121
 122
 123
 124
 125
 126
 127
 128
 129
 130
 131
 132
 133
 134
 135
 136
 137
 138
 139
 140
 141
 142
 143
 144
 145
 146
 147
 148
 149
 150
 151
 152
 153
 154
 155
 156
 157
 158
 159
 160
 161
 162
 163
 164
 165
 166
 167
 168
 169
 170
 171
 172
 173
 174
 175
 176
 177
 178
 179
 180
 181
 182
 183
 184
 185
 186
 187
 188
 189
 190
 191
 192
 193
 194
 195
 196
 197
 198
 199
 200
 201
 202
 203
 204
 205
 206
 207
 208
 209
 210
 211
 212
 213
 214
 215
 216
 217
 218
 219
 220
 221
 222
 223
 224
 225
 226
 227
 228
 229
 230
 231
 232
 233
 234
 235
 236
 237
 238
 239
 240
 241
 242
 243
 244
 245
 246
 247
 248
 249
 250
 251
 252
 253
 254
 255
 256
 257
 258
 259
 260
 261
 262
 263
 264
 265
 266
 267
 268
 269
 270
 271
 272
 273
 274
 275
 276
 277
 278
 279
 280
 281
 282
 283
 284
 285
 286
 287
 288
 289
 290
 291
 292
 293
 294
 295
 296
 297
 298
 299
 300
 301
 302
 303
 304
 305
 306
 307
 308
 309
 310
 311
 312
 313
 314
 315
 316
 317
 318
 319
 320
 321
 322
 323
 324
 325
 326
 327
 328
 329
 330
 331
 332
 333
 334
 335
 336
 337
 338
 339
 340
 341
 342
 343
 344
 345
 346
 347
 348
 349
 350
 351
 352
 353
 354
 355
 356
 357
 358
 359
 360
 361
 362
 363
 364
 365
 366
 367
 368
 369
 370
 371
 372
 373
 374
 375
 376
 377
 378
 379
 380
 381
 382
 383
 384
 385
 386
 387
 388
 389
 390
 391
 392
 393
 394
 395
 396
 397
 398
 399
 400
 401
 402
 403
 404
 405
 406
 407
 408
 409
 410
 411
 412
 413
 414
 415
 416
 417
 418
 419
 420
 421
 422
 423
 424
 425
 426
 427
 428
 429
 430
 431
 432
 433
 434
 435
 436
 437
 438
 439
 440
 441
 442
 443
 444
 445
 446
 447
 448
 449
 450
 451
 452
 453
 454
 455
 456
 457
 458
 459
 460
 461
 462
 463
 464
 465
 466
 467
 468
 469
 470
 471
 472
 473
 474
 475
 476
 477
 478
 479
 480
 481
 482
 483
 484
 485
 486
 487
 488
 489
 490
 491
 492
 493
 494
 495
 496
 497
 498
 499
 500
 501
 502
 503
 504
 505
 506
 507
 508
 509
 510
 511
 512
 513
 514
 515
 516
 517
 518
 519
 520
 521
 522
 523
 524
 525
 526
 527
 528
 529
 530
 531
 532
 533
 534
 535
 536
 537
 538
 539
 540
 541
 542
 543
 544
 545
 546
 547
 548
 549
 550
 551
 552
 553
 554
 555
 556
 557
 558
 559
 560
 561
 562
 563
 564
 565
 566
 567
 568
 569
 570
 571
 572
 573
 574
 575
 576
 577
 578
 579
 580
 581
 582
 583
 584
 585
 586
 587
 588
 589
 590
 591
 592
 593
 594
 595
 596
 597
 598
 599
 600
 601
 602
 603
 604
 605
 606
 607
 608
 609
 610
 611
 612
 613
 614
 615
 616
 617
 618
 619
 620
 621
 622
 623
 624
 625
 626
 627
 628
 629
 630
 631
 632
 633
 634
 635
 636
 637
 638
 639
 640
 641
 642
 643
 644
 645
 646
 647
 648
 649
 650
 651
 652
 653
 654
 655
 656
 657
 658
 659
 660
 661
 662
 663
 664
 665
 666
 667
 668
 669
 670
 671
 672
 673
 674
 675
 676
 677
 678
 679
 680
 681
 682
 683
 684
 685
 686
 687
 688
 689
 690
 691
 692
 693
 694
 695
 696
 697
 698
 699
 700
 701
 702
 703
 704
 705
 706
 707
 708
 709
 710
 711
 712
 713
 714
 715
 716
 717
 718
 719
 720
 721
 722
 723
 724
 725
 726
 727
 728
 729
 730
 731
 732
 733
 734
 735
 736
 737
 738
 739
 740
 741
 742
 743
 744
 745
 746
 747
 748
 749
 750
 751
 752
 753
 754
 755
 756
 757
 758
 759
 760
 761
 762
 763
 764
 765
 766
 767
 768
 769
 770
 771
 772
 773
 774
 775
 776
 777
 778
 779
 780
 781
 782
 783
 784
 785
 786
 787
 788
 789
 790
 791
 792
 793
 794
 795
 796
 797
 798
 799
 800
 801
 802
 803
 804
 805
 806
 807
 808
 809
 810
 811
 812
 813
 814
 815
 816
 817
 818
 819
 820
 821
 822
 823
 824
 825
 826
 827
 828
 829
 830
 831
 832
 833
 834
 835
 836
 837
 838
 839
 840
 841
 842
 843
 844
 845
 846
 847
 848
 849
 850
 851
 852
 853
 854
 855
 856
 857
 858
 859
 860
 861
 862
 863
 864
 865
 866
 867
 868
 869
 870
 871
 872
 873
 874
 875
 876
 877
 878
 879
 880
 881
 882
 883
 884
 885
 886
 887
 888
 889
 890
 891
 892
 893
 894
 895
 896
 897
 898
 899
 900
 901
 902
 903
 904
 905
 906
 907
 908
 909
 910
 911
 912
 913
 914
 915
 916
 917
 918
 919
 920
 921
 922
 923
 924
 925
 926
 927
 928
 929
 930
 931
 932
 933
 934
 935
 936
 937
 938
 939
 940
 941
 942
 943
 944
 945
 946
 947
 948
 949
 950
 951
 952
 953
 954
 955
 956
 957
 958
 959
 960
 961
 962
 963
 964
 965
 966
 967
 968
 969
 970
 971
 972
 973
 974
 975
 976
 977
 978
 979
 980
 981
 982
 983
 984
 985
 986
 987
 988
 989
 990
 991
 992
 993
 994
 995
 996
 997
 998
 999
 1000
 1001
 1002
 1003
 1004
 1005
 1006
 1007
 1008
 1009
 1010
 1011
 1012
 1013
 1014
 1015
 1016
 1017
 1018
 1019
 1020
 1021
 1022
 1023
 1024
 1025
 1026
 1027
 1028
 1029
 1030
 1031
 1032
 1033
 1034
 1035
 1036
 1037
 1038
 1039
 1040
 1041
 1042
 1043
 1044
 1045
 1046
 1047
 1048
 1049
 1050
 1051
 1052
 1053
 1054
 1055
 1056
 1057
 1058
 1059
 1060
 1061
 1062
 1063
 1064
 1065
 1066
 1067
 1068
 1069
 1070
 1071
 1072
 1073
 1074
 1075
 1076
 1077
 1078
 1079
 1080
 1081
 1082
 1083
 1084
 1085
 1086
 1087
 1088
 1089
 1090
 1091
 1092
 1093
 1094
 1095
 1096
 1097
 1098
 1099
 1100
 1101
 1102
 1103
 1104
 1105
 1106
 1107
 1108
 1109
 1110
 1111
 1112
 1113
 1114
 1115
 1116
 1117
 1118
 1119
 1120
 1121
 1122
 1123
 1124
 1125
 1126
 1127
 1128
 1129
 1130
 1131
 1132
 1133
 1134
 1135
 1136
 1137
 1138
 1139
 1140
 1141
 1142
 1143
 1144
 1145
 1146
 1147
 1148
 1149
 1150
 1151
 1152
 1153
 1154
 1155
 1156
 1157
 1158
 1159
 1160
 1161
 1162
 1163
 1164
 1165
 1166
 1167
 1168
 1169
 1170
 1171
 1172
 1173
 1174
 1175
 1176
 1177
 1178
 1179
 1180
 1181
 1182
 1183
 1184
 1185
 1186
 1187
 1188
 1189
 1190
 1191
 1192
 1193
 1194
 1195
 1196
 1197
 1198
 1199
 1200
 1201
 1202
 1203
 1204
 1205
 1206
 1207
 1208
 1209
 1210
 1211
 1212
 1213
 1214
 1215
 1216
 1217
 1218
 1219
 1220
 1221
 1222
 1223
 1224
 1225
 1226
 1227
 1228
 1229
 1230
 1231
 1232
 1233
 1234
 1235
 1236
 1237
 1238
 1239
 1240
 1241
 1242
 1243
 1244
 1245
 1246
 1247
 1248
 1249
 1250
 1251
 1252
 1253
 1254
 1255
 1256
 1257
 1258
 1259
 1260
 1261
 1262
 1263
 1264
 1265
 1266
 1267
 1268
 1269
 1270
 1271
 1272
 1273
 1274
 1275
 1276
 1277
 1278
 1279
 1280
 1281
 1282
 1283
 1284
 1285
 1286
 1287
 1288
 1289
 1290
 1291
 1292
 1293
 1294
 1295
 1296
 1297
 1298
 1299
 1300
 1301
 1302
 1303
 1304
 1305
 1306
 1307
 1308
 1309
 1310
 1311
 1312
 1313
 1314
 1315
 1316
 1317
 1318
 1319
 1320
 1321
 1322
 1323
 1324
 1325
 1326
 1327
 1328
 1329
 1330
 1331
 1332
 1333
 1334
 1335
 1336
 1337
 1338
 1339
 1340
 1341
 1342
 1343
 1344
 1345
 1346
 1347
 1348
 1349
 1350
 1351
 1352
 1353
 1354
 1355
 1356
 1357
 1358
 1359
 1360
 1361
 1362
 1363
 1364
 1365
 1366
 1367
 1368
 1369
 1370
 1371
 1372
 1373
 1374
 1375
 1376
 1377
 1378
 1379
 1380
 1381
 1382
 1383
 1384
 1385
 1386
 1387
 1388
 1389
 1390
 1391

2 in (Defazio et al., 2024)), this bound does not prove convergence. To transform this bound into a convergence theorem, an additional constraint that ties together the learning rates and averaging parameters is required, as we show in Theorem 3.2. When using this new setting for averaging parameters, we refer to the resulting method as `schedulet`. We then specialize our theory to the `wsd` (warmup-stable-decay) schedule and show that `schedulet` achieves the optimal convergence rate of $\mathcal{O}(DG/\sqrt{T})$. We then confirm that our resulting convergence theorem, despite having been established for convex losses, is remarkably good at predicting the behavior of `schedulet` on deep learning tasks. See Figure 1 for a comparison between our theoretical prediction of the loss curve and the empirical loss curve for training a ResNet-20.

Second, we propose a new adaptive learning rate for `schedule-free` based on the Polyak step-size, which we call `schedulep`. We establish the last-iterate convergence of `schedulep`, which achieves an *any-time* (meaning that the total number of iterations is not known in advance) optimal convergence rate of $\mathcal{O}(GD/\sqrt{t})$ for every t for the convex and G -Lipschitz setting. The downside to `schedulep` is that it requires access to the batch loss on the optimal parameters. Fortunately this optimal loss can be reasonably approximated in either the interpolation setting, or the black-box model distillation setting, in which the student (a smaller model) is trained on one of the tasks that the teacher (a larger model) is pretrained. Under this setting, we can obtain an approximation of optimal batch loss of the student by querying the teacher’s loss.

1.1 SCHEDULE-FREE SGD

Consider the stochastic optimization problem

$$\min_{\mathbf{x} \in \mathbb{R}^d} f(\mathbf{x}) := \mathbb{E}_{\mathcal{D}} [f_{\zeta}(\mathbf{x})],$$

where \mathcal{D} is some data distribution over \mathbb{R}^q , $\zeta \in \mathbb{R}^q$ is sampled data from \mathcal{D} , and $f_{\zeta} : \mathbb{R}^d \rightarrow \mathbb{R}$ is our loss function. We assume that $f : \mathbb{R}^d \rightarrow \mathbb{R}$ is convex, G -Lipschitz and that the problem is well-posed, in the sense that a minimizer $\mathbf{x}_* \in \operatorname{argmin}_{\mathbf{x} \in \mathbb{R}^d} f(\mathbf{x})$ exists.

The `schedule-free` has three sets of iterates, the primal averaging iterates \mathbf{y}_t , the offline averaging iterates \mathbf{x}_t , and accumulate gradient iterates \mathbf{z}_t . At iteration t (for $t = 0, 1, \dots, T-1$), we draw a batch of data ζ_t and evaluate the stochastic gradient² $\nabla f(\mathbf{y}_t, \zeta_t)$ at \mathbf{y}_t . At each iteration t , this stochastic gradient is used in the `schedule-free` update as follows

$$\mathbf{y}_t = (1 - \beta_t) \mathbf{z}_{t-1} + \beta_t \mathbf{x}_t \quad (1)$$

$$\mathbf{z}_t = \mathbf{z}_{t-1} - \gamma_t \nabla f(\mathbf{y}_t, \zeta_t) \quad (2)$$

$$\mathbf{x}_{t+1} = (1 - c_{t+1}) \mathbf{x}_t + c_{t+1} \mathbf{z}_t, \quad (3)$$

where $\beta_t \in [0, 1]$ is the *momentum* parameter, $\gamma_t > 0$ is the *learning rate*, and $c_{t+1} \in [0, 1]$ is the *averaging parameter* over \mathbf{x}_t and \mathbf{z}_t . In practice, the method would be implemented with only one additional sequence given by substituting out \mathbf{y}_t as follows

$$\mathbf{z}_t = \mathbf{z}_{t-1} - \gamma_t \nabla f((1 - \beta_t) \mathbf{z}_{t-1} + \beta_t \mathbf{x}_t, \zeta_t) \quad (4)$$

$$\mathbf{x}_{t+1} = (1 - c_{t+1}) \mathbf{x}_t + c_{t+1} \mathbf{z}_t. \quad (5)$$

The momentum parameter β_t interpolates between Polyak-Ruppert averaging when $\beta_t = 0$ and Primal averaging when $\beta_t = 1$. Defazio et al. (2024) suggests that the momentum parameter $\beta_t \equiv \beta \approx 0.9$ works best in practice.

1.2 CONTRIBUTIONS AND BACKGROUND

Schedule-free theory. Defazio et al. (2024) showed `schedule-free` achieves the optimal $\mathcal{O}(DG/\sqrt{T})$ convergence rate for a fixed horizon T in the convex and G -Lipschitz setting with a constant learning rate $\gamma_t \equiv \gamma$ and averaging parameters $c_t = 1/t$ for $t = 1, \dots, T$. Though Defazio et al. (2024) present a more general result in their Theorem 2 that does hold for every c_t and schedule γ_t , their result does not guarantee convergence.

²Formally $\nabla f(\mathbf{y}_t, \zeta_t)$ is a subgradient, since we assumed $f(\mathbf{y}, \zeta)$ is convex in \mathbf{y} , but not necessarily smooth. But for the sake of simplicity we omit this technical detail.

108 The **schedule-free** method is also closely related to the AC-SA algorithm, which also converges
 109 at the optimal rate of $\mathcal{O}(1/\sqrt{T})$ (Lan, 2012, Corollary 1).
 110

111 Recently, Brown (2025) proved the convergence of **schedule-free** in smooth nonconvex setting.
 112 In all of the cases, the author only discussed the momentum parameter being $\beta_t \equiv 1$, which reduces
 113 to the primal averaging. Also, the author considered a constant learning rate $\gamma_t \equiv \gamma$ (or an increasing
 114 learning rate $\gamma_t = \gamma_0(t+1)$) with different choices of c_t for $t = 1, \dots, T$, and established the best-
 115 iterate (in hindsight) convergence to a stationary point.
 116

117 *Contributions.* We provide a convergence theorem for **schedule-free** in the convex Lipschitz
 118 setting that admits any learning rate schedule in Theorem 3.2. To establish this theorem, we require
 119 setting the averaging parameter c_t based on the learning rate via $c_t = \gamma_t / \sum_{k=1}^t \gamma_k$. In the special
 120 case that γ_t is constant, this recovers the $c_t = 1/t$ from Defazio et al. (2024). Our theory can
 121 be applied to the **wsd** schedule, which yields the optimal convergence rate of $\mathcal{O}(DG/\sqrt{T})$, see
 122 Corollary 2.3.
 123

124 **Momentum for Non-smooth Convex Optimization.** Both Tao et al. (2018) and Defazio &
 125 Gower (2021) established that SGD with momentum achieves the optimal last-iterate $\mathcal{O}(1/\sqrt{T})$ con-
 126 vergence rate in the convex and Lipschitz setting with a constant step size.
 127

128 *Contributions.* Because primal averaging is a special case of **schedule-free** when $\beta_t \equiv 1$, and
 129 primal averaging itself is equivalent to **Momentum** (see Sebbouh et al. (2021)), our Theorem 3.2 and
 130 subsequent Corollary 2.3 for **wsd** schedules includes **Momentum** as a special case. Thus we have
 131 extended the convergence of **Momentum** from constant schedules to any schedule.
 132

133 **Convex Theory for Deep Learning.** Surprisingly, convex optimization theory has been shown to
 134 produce practical methods for training large language models. For example, **Adagrad** was developed
 135 based on non-smooth convex analysis and became widely used in deep learning until **RMSprop**
 136 and **Adam** improved upon it (Duchi et al., 2011). Furthermore, a recent work by Schaipp et al.
 137 (2025) has shown that non-smooth convex analysis for SGD can effectively predict the performance
 138 in deep learning. In particular (Schaipp et al., 2025) found that the empirical convergence of **AdamW**
 139 with a **wsd** schedule for large language model training behave similarly to an optimal last-iterate
 140 convergence bound for SGD in non-smooth convex setting (Defazio et al., 2023).
 141

142 *Contributions.* Taking inspiration from Schaipp et al. (2025), we compare our new last-iterate con-
 143 vergence theory of **schedule-free** to the practical convergence on a Resnet-20 for CIFAR10.
 144 Our comparison shows that the theory can predict which schedules will converge, which schedules
 145 will produce spikes with remarkable accuracy, and even when divergence will occur.
 146

147 **Warmup, stable, decay schedule.** The **wsd** schedule consists of three phases: warmup, constant
 148 and cooldown, and hence is also known as the trapezoidal schedule (Zhai et al., 2022). The experi-
 149 ments by Hägele et al. (2024) found that **wsd** performed as good as or even better than the **cosine**
 150 schedule with the cooldown phase. Furthermore, **wsd** is better suited for training foundation models,
 151 where the cooldown phase can be used for finetuning (Hägele et al., 2024).
 152

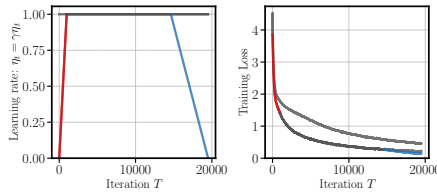
153 *Contributions.* As a special case of our main theorem, we show that, the **schedule-free** SGD
 154 method, applied with the **wsd** schedule, can achieve an optimal convergence rate of $\mathcal{O}(1/\sqrt{T})$.
 155

156 **Polyak Stepsize.** The Polyak stepsize was first introduced by Polyak (1987) in the deterministic
 157 setting, where the convergence was proved for the non-smooth and convex setting. Hazan & Kakade
 158 (2019) revisited the Polyak stepsize for the class of gradient descent methods and showed that Polyak
 159 stepsize has near-optimal convergence rate in the Lipschitz, smooth, and strongly convex setting
 160 without accessing to any of the Lipschitz, smoothness or strong convexity parameters.
 161

162 Recently, there have been many proposals of a stochastic Polyak stepsize in machine learning; see
 163 (Berrada et al., 2020; Loizou et al., 2021). Assuming access to $f_\zeta(\mathbf{x}_*)$, the **SPS*** by Gower et al.
 164 (2025) achieves the best known rates across several classes of convex functions. Moreover, Gower
 165 et al. (2025) proposed an adaptive Polyak stochastic stepsize, called **IAM** (Iterate Averaging Adap-
 166 tive method), for the momentum method. Other variants of stochastic Polyak with momentum in-
 167 clude (Oikonomou & Loizou, 2024; Wang et al., 2023; Orvieto & Xiao, 2024).
 168

162 *Contributions.* We suggest a Polyak stepsize for `schedule-free`. With an arbitrary choice of the
 163 momentum parameter $\beta_t \equiv \beta \in [0, 1]$, we prove an optimal *anytime* last-iterate convergence bound
 164 of $\mathcal{O}(GD/\sqrt{t})$ for every t for the non-smooth convex setting in Theorem 3.2. We then consider
 165 the application black-box model distillation setting proposed by Gower et al. (2025), and show
 166 that our new Polyak stepsize for `schedule-free` achieves strong performance compared to several
 167 benchmark methods on both the TinyShakespeare and fineweb1B data set.

2 CONVERGENCE ANALYSIS AND IMPLICATIONS



171
 172
 173
 174
 175
 176
 177
 178
 179 Figure 2: Training loss for
 180 `schedule-free` on ResNet-20
 181 /Cifar10 with a constant learning
 182 rate schedule (gray), warmup-stable (red-
 183 gray), and wsdl schedule (red-gray-blue).

The `schedule-free` algorithm was designed to perform well without the need to tune additional hyperparameters beyond momentum. For convex and Lipschitz objectives, it achieves the optimal convergence guarantees with a constant step size. Despite this, `schedule-free` is used with a linear warmup schedule, which the authors note is necessary for competitive performance. This added benefit over a constant schedule is demonstrated in Figure 2 for a small deep learning model. This indicates a gap between theory and practice, which motivates a natural question: Does `schedule-free` remain optimal with a non-constant schedule, in the convex setting?

184 We begin by stating our convergence result for the `schedule-free` SGD method with a general,
 185 non-constant learning rate in Theorem 2.1. The proof of the theorem is deferred to Appendix A.

187 **Theorem 2.1.** Let $f: \mathbb{R}^d \rightarrow \mathbb{R}$ be convex and G -Lipschitz continuous. Let $\{\mathbf{x}_t, \mathbf{y}_t, \mathbf{z}_t\}$ be generated
 188 from (1), (2), (3). Suppose that

$$c_t = \frac{\gamma_t}{\sum_{i=0}^t \gamma_i} \quad (6)$$

191 for $t = 1, \dots, T$. Initializing $\mathbf{z}_{-1} = \mathbf{x}_0$, we then have

$$\mathbb{E}[f(\mathbf{x}_T) - f(\mathbf{x}_*)] \leq \frac{\frac{1}{2}\|\mathbf{x}_0 - \mathbf{x}_*\|^2 + \gamma_0(f(\mathbf{x}_0) - f(\mathbf{x}_*))}{\sum_{t=0}^T \gamma_t} + \sum_{t=0}^T \frac{\frac{1}{2}\gamma_t^2 G^2}{\sum_{t=0}^T \gamma_t}. \quad (7)$$

196 Our theory shows a last-iterate convergence bound for the `schedule-free` SGD method with
 197 general learning rates. First, for $D := \|\mathbf{x}_0 - \mathbf{x}_*\|$, we can see that by choosing $\gamma_t \equiv \frac{D}{G\sqrt{T}}$ for all t ,
 198 we recover the optimal $\mathcal{O}(DG/\sqrt{T})$ convergence rate given in Theorem 1 in Defazio et al. (2024).
 199 Moreover, for non-constant learning rates, Theorem 2.1 suggests a theoretically well-motivated aver-
 200 aging parameter c_t that is set based on all the past learning rates $\{\gamma_0, \dots, \gamma_t\}$. This choice of c_t
 201 in (6) is similar to the heuristic choice of $c_{t+1} = \frac{\gamma_t^2}{\sum_{i=0}^t \gamma_i^2}$ suggested by Defazio et al. (2024, equation
 202 (23)). This heuristic choice is the default setting in the code base³ for `schedule-free`.

203 A natural question is, why should we care about this theoretical convergence theory which holds only
 204 for convex functions, whereas `schedule-free` is a method for non-convex deep learning? Towards
 205 answering this question, we perform several experiments comparing the predicted convergence of
 206 this theorem, to the practical convergence for training a neural network in the following section.

2.1 SURPRISING PREDICTIVE POWER FOR DEEP LEARNING

211 Inspired by Schaipp et al. (2025), we compute our last-iterate convergence bound from Theorem 2.1
 212 and compare it to the empirical performance of `schedule-free` on ResNet-20/Cifar10 for
 213 wsdl schedule with cooldown starting at $\{0.25T, 0.5T, 0.75T\}$ where T is the training horizon. We
 214 outline the experiment setup and present a comparison using the cosine schedule in Appendix E.

215
 3³https://github.com/facebookresearch/schedule_free

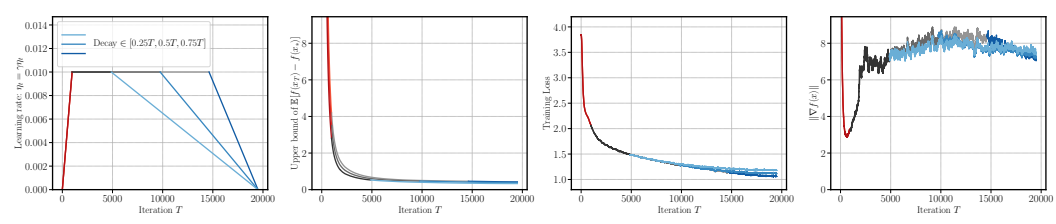


Figure 3: Using `wsd` schedules with three different cooldown periods and with base learning rate $\gamma = 0.01$, our plots compare the theoretical convergence (Theorem 2.1) to the empirical convergence of ResNet-20/Cifar10, with the gradient norm shown for reference. The red color denotes the warmup period, the gray color denotes the constant period, and the blue color denotes the cooldown period.

We take \mathbf{x}_* to be the iterate with the smallest loss $f(\mathbf{x}_*)$ during training. In Figures 1 and 3, we use the `wsd` schedule with a large ($\gamma = 10$) and small ($\gamma = 0.01$) base learning rate, respectively.

For a small base learning rate, the theory predicts the convergence seen in practice across all three cooldown schedules, see Figure 3. For a large base learning rate, the theory predicts the transient spikes in the loss regardless whether it occurs *before* or *after* the cooldown period, see Figure 1. One possible explanation is that, the spikes are caused by the spikes in the gradient norm (see the rightmost figure in Figure 1). Yet, one should also note that our theory predicts the convergence in Figure 3 even with the blowup of the gradient norms. Finally, in Figure 4, using a constant-then-diverging schedule, our theory also predicts all spikes in the loss, and whether and when the training diverges.

These experiments show a striking similarity between the convex theory bounds and the loss curves observed in the non-convex setting. Having established that our theory has some predictive power for deep learning, we now specialize our theory to the `wsd` schedule.

2.2 APPLICATION TO `wsd` SCHEDULE

The `wsd` schedule (warmup-stable-decay), a trapezoidal shape learning rate schedule, has been shown to be very useful for training large language models (Hägle et al., 2024). For this section we divide the learning rate into

$$\gamma_t = \gamma \eta_t$$

where $\gamma > 0$ is the *base learning rate*, which is the parameter that is tuned, and η_t is the *schedule*. For `wsd` there are three phases of the schedule: first, a warmup period, then a constant period, and at last, a cooldown period. Formally, for $0 \leq T_w \leq T_c \leq T$, the `wsd` schedule is given by:

$$\eta_t = \begin{cases} \frac{t+1}{T_w+1}, & \text{if } 0 \leq t \leq T_w, \\ 1, & \text{if } T_w < t \leq T_c, \\ \frac{T-t+1}{T-T_c+1}, & \text{if } T_c < t \leq T. \end{cases} \quad (8)$$

Substituting the `wsd` schedule (8) into (6), we can obtain a sequence of averaging parameters.

Lemma 2.2. Let $0 \leq T_w \leq T_c \leq T$ and $\gamma > 0$. Suppose that $\{\eta_t\}_{t=0}^T$ follows the `wsd` schedule given in (8). We can determine $\{c_t\}_{t=0}^T$ by

$$c_t = \begin{cases} \frac{2}{t+2}, & \text{if } 0 \leq t \leq T_w, \\ \frac{2}{2t-T_w+2}, & \text{if } T_w < t \leq T_c, \\ \frac{2(T-t+1)}{(T-T_c+1)(2T_c-T_w+2)+(2T-T_c-t+1)(t-T_c)}, & \text{if } T_c < t \leq T. \end{cases} \quad (9)$$

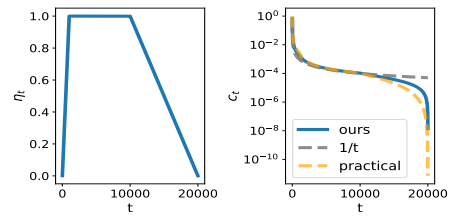


Figure 5: The averaging parameter c_t when applied with the `wsd` schedule where blue is our proposed $c_t = \eta_t / \sum_{i=0}^t \eta_i$, gray is $c_t = 1/t$, and the orange is the practical heuristic $c_t = \eta_t^2 / \sum_{i=0}^t \eta_i^2$.

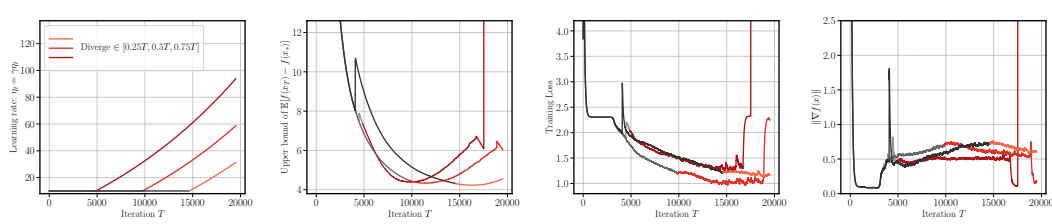


Figure 4: Using schedules with three three different diverging periods, we compare the theoretical convergence given by Theorem 2.1 to the empirical convergence of ResNet-20/Cifar10. The gray color denotes the constant period and the red color denotes the diverging period.

To illustrate the results in Lemma 2.2, Figure 5 plots the resulting averaging parameters c_t when applied a `wsd` schedule. The blue line, the gray dashed line, and the orange dashed line depict our proposed c_t in (9), the theoretical $c_t = 1/t$, and the practical default $c_{t+1} = \frac{\gamma_t^2}{\sum_{i=0}^t \gamma_i^2}$ for `schedule-free` (Defazio et al., 2024, Algorithm 1), respectively. As can be seen, our theoretically motivated choice is close to the default practical choice proposed in Defazio et al. (2024), particularly as t grows. Using the `wsd` schedule η_t defined in (8) and the weights c_t given in (9), we obtain the convergence result in Corollary 2.3.

Corollary 2.3 shows that, the `schedule-free` SGD with the `wsd` schedule achieves an optimal convergence rate of $\mathcal{O}(1/\sqrt{T})$ as long as the base learning rate is well-chosen.

Corollary 2.3. Let $D = \|\mathbf{x}_0 - \mathbf{x}_\star\|$. Using the `wsd` parameters (c_t, η_t) given in (9) and (8), with a base learning rate of $\gamma = \frac{D}{G\sqrt{\sum_{t=0}^T \eta_t^2}}$, we have the convergence

$$\mathbb{E}[f(\mathbf{x}_T) - \inf f] \leq \frac{2\eta_0(f(\mathbf{x}_0) - f(\mathbf{x}_\star))}{T + T_c - T_w + 2} + \frac{2\sqrt{\frac{2}{3}}DG}{\sqrt{T + T_c - T_w + 2}} \simeq \mathcal{O}\left(\frac{DG}{\sqrt{T}}\right). \quad (10)$$

3 POLYAK LEARNING RATE

Having seen that using convexity as an assumption can result in theory with some predictive power on neural network experiments, in this section, we use convexity to design an adaptive learning rate schedule, which we call `schedulep`, see Algorithm 1 for the pseudo-code. Here, we denote $(\cdot)_+^2 = ((\cdot)_+)^2$; i.e., $(a)_+^2 = a^2$ if $a > 0$ and $(a)_+^2 = 0$ otherwise.

To derive this adaptive stepsizes, we make use of the following *Interpolation* assumption.

Assumption 3.1 (Interpolation). For every ζ , we have access to $f_\zeta(\mathbf{x}_\star)$ where $\mathbf{x}_\star \in \operatorname{argmin}_{\mathbf{x} \in \mathbb{R}^d} f(\mathbf{x})$.

We call this the interpolation assumption, because it holds for models that interpolate the data, in which case $f_\zeta(\mathbf{x}_\star) = 0$ since every data point has a perfect fit, and thus zero loss (Ma et al., 2018; Liu et al., 2022; Gower et al., 2021). Many vision models interpolate the data, unlike language models which have a strictly positive entropy rate: the next word in a sequence is never perfectly predictable (Shannon, 1948; Cover & King, 1978). Though one can still approximate $f_\zeta(\mathbf{x}_\star)$ for language models, see Section 4.2.

Algorithm 1 Schedulep: Schedule-free Polyak

```

1: Input:  $\mathbf{z}_{-1} = \mathbf{x}_0 \in \mathbb{R}^d, \beta \in [0, 1], c_t > 0, \gamma_{\max} > 0$ .
2: for  $t = 0$  to  $T - 1$  do
3:    $\mathbf{y}_t = (1 - \beta)\mathbf{z}_{t-1} + \beta\mathbf{x}_t$ 
4:    $\tau_t = \frac{[f_{\zeta_t}(\mathbf{y}_t) - f_{\zeta_t}(\mathbf{x}_\star) + \beta(\nabla f(\mathbf{y}_t, \zeta_t), \mathbf{z}_{t-1} - \mathbf{x}_t)]_+}{\|\nabla f(\mathbf{y}_t, \zeta_t)\|^2}$ 
5:    $\gamma_t = \min\{\gamma_{\max}, \tau_t\}$ 
6:    $\mathbf{z}_t = \mathbf{z}_{t-1} - \gamma_t \nabla f(\mathbf{y}_t, \zeta_t)$ 
7:    $\mathbf{x}_{t+1} = (1 - c_{t+1})\mathbf{x}_t + c_{t+1}\mathbf{z}_t$ 
8: end for
9: Return:  $\mathbf{x}_T$ 

```

We derive our adaptive learning rate by choosing γ_t that will bring iterate z_t closer to the solution \mathbf{x}_* . For this note from (2) (or equivalently line 1 in Algorithm 1), the iterate z_t explicitly depends on the learning rate γ_t . Consequently we can write $z_t(\gamma_t) \equiv z_t$. We then derive an upper bound on $\|z_t(\gamma_t) - \mathbf{x}_*\|^2$ that only depends on known quantities and $f_{\zeta_t}(\mathbf{x}_*)$ by assuming that the loss function is convex. Minimizing this upper bound in γ_t gives our adaptive learning rate on line 1 in Algorithm 1. We call our resulting algorithm **schedulep** (**schedule-free** with a Polyak learning rate), since this is a generalization of the Polyak learning rate to **schedule-free**. We include this additional cap of γ_{\max} on line 1 in Algorithm 1 to improve stability, specially in the case where $f_{\zeta_t}(\mathbf{x}_*)$ is misspecified. This is a common safe-guard used in stochastic Polyak methods (Loizou et al., 2020).

Next we prove the convergence of our **schedulep** method.

Theorem 3.2. Consider the iterates of Algorithm 1 with $c_t = 1/(t + 1)$, $\beta \in [0, 1)$ and $\gamma_{\max} = \infty$. Let $f_{\zeta} : \mathbb{R}^d \rightarrow \mathbb{R}$ be a convex function for every ζ . Let

$$B := \{\mathbf{x} : \|\mathbf{x} - \mathbf{x}_*\| \leq \|\mathbf{x}_0 - \mathbf{x}_*\|\} \subset \mathbb{R}^d, \quad (11)$$

$$G^2 := \max_{\mathbf{x} \in B} \mathbb{E}_{\zeta} \|\nabla f(\mathbf{x}, \zeta)\|^2. \quad (12)$$

With the initialization $z_{-1} = \mathbf{x}_0$, the suboptimality gap of the *last iterate* \mathbf{x}_t converges at a $1/\sqrt{t}$ rate according to

$$\mathbb{E}[f(\mathbf{x}_t) - f(\mathbf{x}_*)] \leq \frac{G\|\mathbf{x}_0 - \mathbf{x}_*\|}{\sqrt{t+1}}. \quad (13)$$

The resulting rate of convergence of **schedulep** in (13) is exactly the optimal rate for the class of convex and G -Lipschitz functions. Furthermore, this convergence has two additional benefits. First, it is an *anytime* result, in that (13) achieves the optimal rate for every t , where-as previous results for **schedule-free** only achieve the optimal $\mathcal{O}(1/\sqrt{T})$ with the known stopping time T . Second, we do not need to assume that the loss is globally Lipschitz. Rather, that it is Lipschitz in the closed ball given in (11). Thus we are also able to weaken the global Lipschitz assumption.

4 EXPERIMENTS

Our theory suggests a new choice of c_t , which we evaluate against the practical heuristic $c_{t+1} = \gamma_t^2 / \sum_{i=1}^t \gamma_i^2$ and that of the previous theory, $c_t = 1/t$. We run experiments from small- to large-scale across domains (vision and language) and learning tasks (regression, classification, and knowledge distillation). For regression and image classification, we use the SGD variant of **schedule-free**; for distillation in language modeling, we use the **AdamW-schedulefree** variant in Defazio et al. (2024). We use the momentum parameter $\beta = 0.9$ throughout our experiments.

4.1 IMAGE CLASSIFICATION

We test **schedulet** on image classification with Wide Resnet (16-8) on CIFAR10 and DenseNet on CIFAR100. Hyperparameter settings follow that of Defazio et al. (2024), with exact settings listed in Appendix E and Table 1. We compare the performance of **schedule-free** with **schedulet**, the practical heuristic $c_{t+1} = \gamma_t^2 / \sum_{i=1}^t \gamma_i^2$, $c_t = 1/t$ from previous theory, and SGD-m (stochastic gradient descent with momentum). We apply the warmup-stable schedule for **schedule-free** with the practical heuristic averaging parameters and the **wsd** schedule otherwise. We use a 5% warmup for all schedules, and set the cooldown in **wsd** to 25% in smaller models and 5% for larger models. For each model, we sweep the learning rate over a grid for all optimizers, tuning each method using the validation loss as a proxy for generalization ability of the optimizer.

As mentioned in Defazio et al. (2024), **schedule-free** requires batch statistics computed from the \mathbf{x} sequence (i.e. Equation 3) for models using BatchNorm layers. We avoid this complication by using GroupNorm layers for all models, which does not significantly effect the performance and training dynamics of these relatively smaller models.

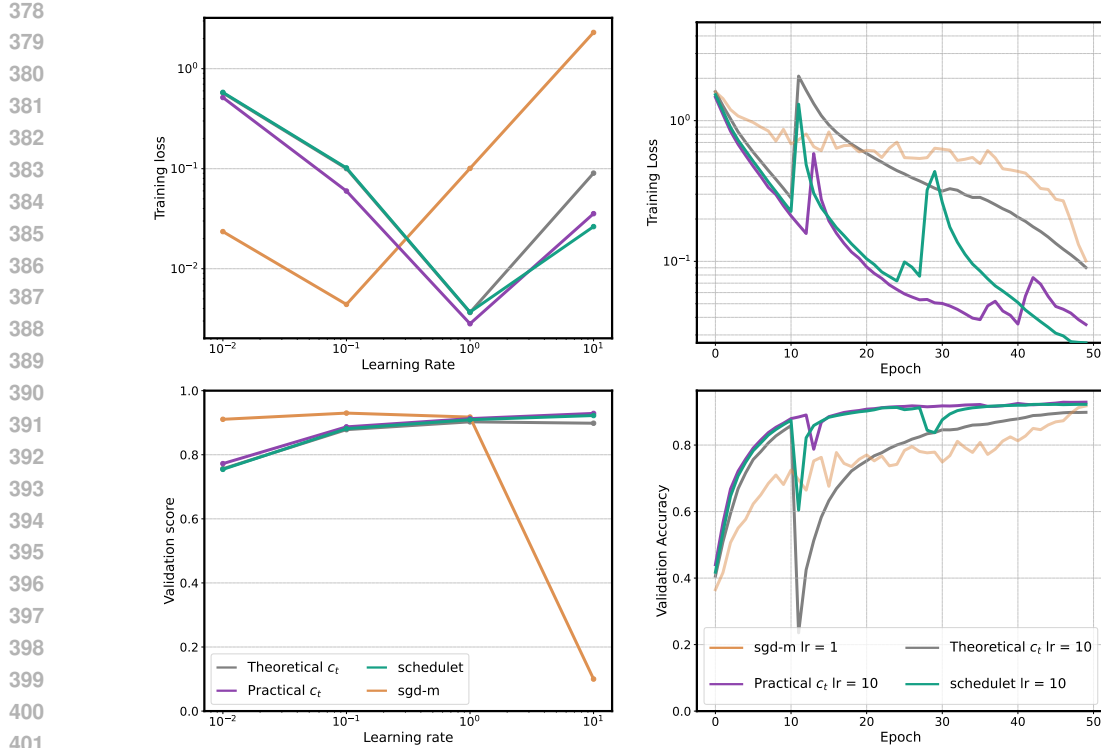


Figure 6: Training a Wide ResNet (16-8) model on the CIFAR10 data set.

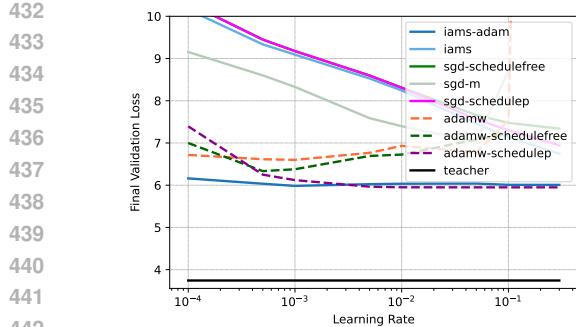
The results in Figure 6 show that, although the practical heuristic averaging parameter generally achieves a smaller training loss than `schedulelet` across different learning rates, their performance are similar in terms of generalization. Moreover, we see that `schedule-free` with different averaging parameters is robust across different learning rates in terms of validation score. When considering the best tuned learning rate ($\gamma = 1$ for SGD-m and $\gamma = 10$ for `schedule-free`), we see that `schedule-free` with the practical heuristic c_t performs slightly better than `schedulelet` in terms of training loss, but as well with respect to validation score. Yet, they both outperform the choice of $c_t = 1/t$ from previous theory. When training larger models, our experiments show that `schedulelet` has similar performance as the practical heuristic parameter; see Figure 10 in Appendix E.1.2.

4.2 MODEL DISTILLATION

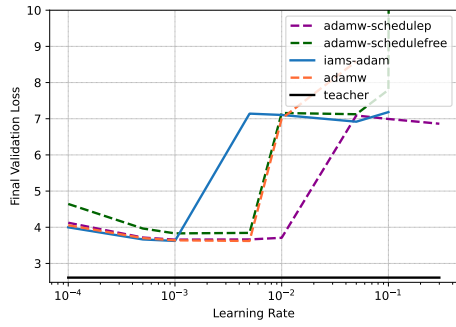
Here we test `Schedulep` in Algorithm 1 on black-box model distillation, where we have only access to the teacher’s loss over a given batch. We will use the teacher’s loss as an approximation of the optimal student’s loss. That is, let f_ζ^t and $f_\zeta^s(x)$ denote the teacher’s loss and the student’s loss with weights x , respectively, for a given batch ζ . We will choose a teacher that has been trained on a large corpora, such that $f_\zeta^t \approx f_\zeta^s(x_*)$, where x_* are the optimal parameters for the student model.

Our setup is based on the experiments by Gower et al. (2025). As a baseline, we used SGD-m, AdamW (Kingma & Ba, 2014), (AdamW-)ScheduleFree (Defazio et al., 2024), and IAMS(-Adam) (Gower et al., 2025). We also test the AdamW version of `Schedulep` called AdamW-Schedulep, see Appendix C and Algorithm 2 for details. For the distillation experiments, we considered two settings:

Distilling `tiny_shakespeare`. The teacher model employed was `gpt2-medium` (345 million parameters), a pre-trained transformer model from the Hugging Face library (Radford et al., 2019). We used a student model with 67.7 million parameters, see Table 2 in Appendix E.2 for details. The results in Figure 7 show that our AdamW-Schedulep achieves the best loss for a tuned



443 Figure 7: Training a smaller student model on the `tiny_shakespeare` data set, using
444 `gpt2-medium` as the teacher.
445



457 Figure 8: Training a nanoGPT student model on the `fineweb1B` data set, using
458 `EleutherAI/gpt-j-6B` as the teacher.
459
460

461 learning rate γ_{\max} , but it is not quite as robust as the IAMS-Adam method is to the choice of learning
462 rate.
463

464 **Distilling fineweb1B.** The teacher model employed was EleutherAI/gpt-j-6B, a 6-
465 billion parameter transformer model pre-trained on diverse datasets (Wang & Komatsuzaki, 2021).
466 We used a nanoGPT model with 124 million parameters as the student, see Table 2 in Appendix E.2
467 for details, and Figure 8 shows AdamW-Schedulep is now the most robust method with respect to
468 different choices of learning rate γ_{\max} , but the best loss is achieved by tuning AdamW or IAMS-Adam.
469

470 5 CONCLUSION AND LIMITATIONS

471 We developed the last-iterate convergence theory for `schedule-free` that works for general non-
472 constant schedule in the convex Lipschitz setting. The theory requires the averaging parameter to be
473 a function of the learning rate schedule, which we called `schedulet`. We showed that our theory is
474 good at predicting the empirical behavior of `schedulet`. We also obtained the optimal convergence
475 $\mathcal{O}(GD/\sqrt{T})$ from the theory when specialized to `wsd` schedule. Next, assuming convexity and in-
476 terpolation, we developed a Polyak stepsize for `schedule-free`, called `schedulep`. We proved an
477 any-time convergence $\mathcal{O}(GD/\sqrt{t})$ for `schedulep` and demonstrated its strong performance com-
478 pared to several benchmark methods under the black-box distillation model setting.
479

480 The limitation of our work is that, our theory only applies for general learning rate schedule with
481 `schedulet`, so it does not give any convergence bounds for the averaging parameter used in practice.
482 In fact, our suggested averaging parameter schedule does not improve the training performance in
483 practice. Moreover, our comparison between the convergence theory and the empirical performance
484 is via visual inspection but not a quantitative analysis. For the Polyak stepsize `schedulep`, it can
485 only be applied to models that nearly interpolate the data or under the black-box model distillation
setting.

486 **Reproducibility Statement.** To ensure reproducibility, we provide our open-source repository
 487 built upon publicly available implementations of common vision and language models, optimiz-
 488 ers, and training frameworks. We extend the open-source framework `step-back`⁴ to incorpo-
 489 rate `Schedule-free`⁵, `Wide ResNet`⁶ and `DenseNet`⁷ architectures with GroupNorm layers.
 490 Complete training specifications, architectures, and hyperparameters are detailed in Tables 1–2 and
 491 Appendix E.

492
 493 **REFERENCES**
 494

495 Leonard Berrada, Andrew Zisserman, and M Pawan Kumar. Training neural networks for and by
 496 interpolation. In *International conference on machine learning*, pp. 799–809. PMLR, 2020.

497 Connor Brown. Analysis of schedule-free nonconvex optimization. *arXiv preprint*
 498 *arXiv:2508.06743*, 2025.

499 Thomas M. Cover and Joy A. King. A convergent gambling estimate of the entropy of english. *IEEE*
 500 *Transactions on Information Theory*, 24(4):413–421, 1978.

501 Tri Dao, Daniel Y Fu, Stefano Ermon, Atri Rudra, and Christopher Ré. Flashattention: Fast and
 502 memory-efficient exact attention with io-awareness. In *Advances in Neural Information Process-
 503 ing Systems*, 2022.

504 Aaron Defazio and Robert M Gower. The power of factorial powers: New parameter settings for
 505 (stochastic) optimization. In *Asian Conference on Machine Learning*, pp. 49–64. PMLR, 2021.

506 Aaron Defazio, Ashok Cutkosky, Harsh Mehta, and Konstantin Mishchenko. Optimal linear decay
 507 learning rate schedules and further refinements, 2023. URL <https://arxiv.org/abs/2310.07831>. arXiv preprint.

508 Aaron Defazio, Xingyu Yang, Ahmed Khaled, Konstantin Mishchenko, Harsh Mehta, and Ashok
 509 Cutkosky. The road less scheduled. *Advances in Neural Information Processing Systems*, 37:
 510 9974–10007, 2024.

511 John Duchi, Elad Hazan, and Yoram Singer. Adaptive subgradient methods for online learning and
 512 stochastic optimization. *Journal of machine learning research*, 12(7), 2011.

513 Robert Gower, Othmane Sebbouh, and Nicolas Loizou. SGD for structured nonconvex functions:
 514 Learning rates, minibatching and interpolation. In *Proceedings of The 24th International Con-
 515 ference on Artificial Intelligence and Statistics*, volume 130 of *Proceedings of Machine Learning
 516 Research*, pp. 1315–1323. PMLR, 13–15 Apr 2021.

517 Robert M. Gower, Guillaume Garrigos, Nicolas Loizou, Dimitris Oikonomou, Konstantin
 518 Mishchenko, and Fabian Schaipp. Analysis of an idealized stochastic polyak method and its
 519 application to black-box model distillation, 2025. URL <https://arxiv.org/abs/2504.01898>.

520 Alex Hägele, Elie Bakouch, Atli Kosson, Leandro Von Werra, Martin Jaggi, et al. Scaling laws
 521 and compute-optimal training beyond fixed training durations. *Advances in Neural Information
 522 Processing Systems*, 37:76232–76264, 2024.

523 Elad Hazan and Sham Kakade. Revisiting the polyak step size. *arXiv preprint arXiv:1905.00313*,
 524 2019.

525 Diederik P. Kingma and Jimmy Ba. Adam: A method for stochastic optimization.
 526 *CoRR*, abs/1412.6980, 2014. URL <https://api.semanticscholar.org/CorpusID:6628106>.

527 ⁴<https://github.com/fabian-sp/step-back>

528 ⁵https://github.com/facebookresearch/schedule_free/tree/main

529 ⁶<https://github.com/pytorch/vision/blob/main/torchvision/models/resnet.py>

530 ⁷<https://github.com/weiaicunzai/pytorch-cifar100/blob/master/models/densenet.py>

540 Guanghui Lan. An optimal method for stochastic composite optimization. *Mathematical Programming*,
 541 133(1):365–397, 2012.
 542

543 Chaoyue Liu, Libin Zhu, and Mikhail Belkin. Loss landscapes and optimization in over-
 544 parameterized non-linear systems and neural networks. *Applied and Computational Harmonic
 545 Analysis*, 59:85–116, 2022.

546 Nicolas Loizou, Sharan Vaswani, Issam Laradji, and Simon Lacoste-Julien. Stochastic polyak step-
 547 size for sgd: An adaptive learning rate for fast convergence. *arXiv:2002.10542*, 2020.
 548

549 Nicolas Loizou, Sharan Vaswani, Issam Hadj Laradji, and Simon Lacoste-Julien. Stochastic polyak
 550 step-size for sgd: An adaptive learning rate for fast convergence. In *International Conference on
 551 Artificial Intelligence and Statistics*, pp. 1306–1314. PMLR, 2021.
 552

553 Siyuan Ma, Raef Bassily, and Mikhail Belkin. The power of interpolation: Understanding the effec-
 554 tiveness of SGD in modern over-parametrized learning. In *Proceedings of the 35th International
 555 Conference on Machine Learning*, volume 80 of *Proceedings of Machine Learning Research*, pp.
 556 3325–3334. PMLR, 10–15 Jul 2018.

557 Dimitris Oikonomou and Nicolas Loizou. Stochastic Polyak step-sizes and momentum: Conver-
 558 gence guarantees and practical performance. *arXiv preprint arXiv:2406.04142*, 2024.
 559

560 Antonio Orvieto and Lin Xiao. An adaptive stochastic gradient method with non-negative Gauss-
 561 Newton stepsizes, 2024.
 562

563 Boris T Polyak. *Introduction to optimization*. New York, Optimization Software, 1987.
 564

565 Alec Radford, Jeffrey Wu, Dario Amodei, Jack Clark, et al. Language models are unsupervised
 566 multitask learners. *OpenAI Blog*, 2019.

567 Fabian Schaipp, Alexander Hägele, Adrien Taylor, Umut Simsekli, and Francis Bach. The sur-
 568 prising agreement between convex optimization theory and learning-rate scheduling for large
 569 model training. In *Forty-second International Conference on Machine Learning*, 2025. URL
 570 `https://openreview.net/forum?id=b836TGkRSw`.
 571

572 Othmane Sebbouh, Robert M Gower, and Aaron Defazio. Almost sure convergence rates for stochas-
 573 tic gradient descent and stochastic heavy ball. In Mikhail Belkin and Samory Kpotufe (eds.),
 574 *Proceedings of Thirty Fourth Conference on Learning Theory*, volume 134 of *Proceedings of
 575 Machine Learning Research*, pp. 3935–3971. PMLR, 15–19 Aug 2021.
 576

577 Claude E. Shannon. A mathematical theory of communication. *Bell System Technical Journal*, 27
 578 (3):379–423, 1948.
 579

580 Wei Tao, Zhisong Pan, Gaowei Wu, and Qing Tao. Primal averaging: A new gradient evaluation step
 581 to attain the optimal individual convergence. *IEEE transactions on cybernetics*, 50(2):835–845,
 582 2018.

583 Ben Wang and Aran Komatsuzaki. Gpt-j: An open-source 6b parameter lan-
 584 guage model. *EleutherAI*, 2021. URL `https://github.com/kingoflolz/mesh-transformer-jax`.
 585

586 Xiaoyu Wang, Mikael Johansson, and Tong Zhang. Generalized Polyak step size for first order
 587 optimization with momentum. In *Proceedings of the 40th International Conference on Machine
 588 Learning*, volume 202 of *Proceedings of Machine Learning Research*, pp. 35836–35863. PMLR,
 589 23–29 Jul 2023.
 590

591 Xiaohua Zhai, Alexander Kolesnikov, Neil Houlsby, and Lucas Beyer. Scaling vision transformers.
 592 In *Proceedings of the IEEE/CVF conference on computer vision and pattern recognition*, pp.
 593 12104–12113, 2022.

594	CONTENTS	
595		
596		
597	1 Introduction	1
598	1.1 schedule-free SGD	2
599	1.2 Contributions and Background	2
600		
601		
602	2 Convergence Analysis and Implications	4
603	2.1 Surprising Predictive Power for Deep Learning	4
604	2.2 Application to wsd Schedule	5
605		
606		
607	3 Polyak learning rate	6
608		
609	4 Experiments	7
610	4.1 Image Classification	7
611	4.2 Model Distillation	8
612		
613		
614	5 Conclusion and Limitations	9
615		
616		
617	A Convergence Theory for schedule-free SGD	12
618	A.1 Auxiliary Lemmas	12
619	A.2 Proof of Theorem 2.1	15
620	A.3 Proof of Lemma 2.2	16
621	A.4 Proof of Corollary 2.3	16
622	A.5 Comments on the Weights c_t in Defazio et al. (2024)	18
623		
624		
625		
626	B Proofs for Polyak Step size	19
627	B.1 Derivation of the schedulep learning rate	19
628	B.2 Auxiliary Lemmas	20
629	B.3 Proof of Theorem 3.2	22
630		
631		
632	C Practical & Adam Versions of Schedulep	23
633		
634		
635	D Implications to Momentum Method	24
636		
637	E Experiments: Supplementary Material	27
638	E.1 Image Classification	27
639	E.1.1 Predictive Power for Deep Learning	27
640	E.1.2 Stability Analysis	29
641	E.2 Black-Box Distillation details	30
642		
643		
644		
645	A CONVERGENCE THEORY FOR SCHEDULE-FREE SGD	
646		
647	A.1 AUXILIARY LEMMAS	

648
649
650

Lemma A.1. Let $\{\mathbf{x}_t, \mathbf{y}_t, \mathbf{z}_t\}$ be generated from (1), (2), (3). For $t = 0, 1, \dots, T-1$, we have the following inequality holds:

651
652
653

$$\frac{1}{c_{t+1}} f(\mathbf{x}_{t+1}) - \left(\frac{1}{c_{t+1}} - 1 \right) f(\mathbf{x}_t) - f(\mathbf{x}_*) \leq \langle \nabla f(\mathbf{y}_{t+1}), \mathbf{z}_t - \mathbf{x}_* \rangle \quad (14)$$

654
655

Proof. Dividing both sides of (3) by c_{t+1} and rearranging terms, we have

656
657
658

$$\left(\frac{1}{c_{t+1}} - 1 \right) (\mathbf{x}_{t+1} - \mathbf{x}_t) = \mathbf{z}_t - \mathbf{x}_{t+1}; \quad (15)$$

659

and also (1) implies

660
661
662

$$\mathbf{z}_t - \mathbf{y}_{t+1} = \frac{\beta_{t+1}}{1 - \beta_{t+1}} (\mathbf{y}_{t+1} - \mathbf{x}_{t+1}), \quad (16)$$

663
664

for $t = 0, 1, \dots, T-1$. Applying (15) and (16) and the fact that f is convex, we then obtain

665
666
667
668
669
670
671
672
673
674
675
676
677

$$\begin{aligned} \frac{1}{c_{t+1}} f(\mathbf{x}_{t+1}) - \left(\frac{1}{c_{t+1}} - 1 \right) f(\mathbf{x}_t) - f(\mathbf{x}_*) \\ = \left(\frac{1}{c_{t+1}} - 1 \right) (f(\mathbf{x}_{t+1}) - f(\mathbf{x}_t)) + (f(\mathbf{x}_{t+1}) - f(\mathbf{x}_*)) \\ \leq \left(\frac{1}{c_{t+1}} - 1 \right) \langle \nabla f(\mathbf{x}_{t+1}), \mathbf{x}_{t+1} - \mathbf{x}_t \rangle + (f(\mathbf{x}_{t+1}) - f(\mathbf{x}_*)) \\ \stackrel{(15)}{=} \langle \nabla f(\mathbf{x}_{t+1}), \mathbf{z}_t - \mathbf{x}_{t+1} \rangle + (f(\mathbf{x}_{t+1}) - f(\mathbf{y}_{t+1})) + (f(\mathbf{y}_{t+1}) - f(\mathbf{x}_*)) \\ \leq \langle \nabla f(\mathbf{x}_{t+1}), \mathbf{z}_t - \mathbf{x}_{t+1} \rangle + \langle \nabla f(\mathbf{x}_{t+1}), \mathbf{x}_{t+1} - \mathbf{y}_{t+1} \rangle + \langle \nabla f(\mathbf{y}_{t+1}), \mathbf{y}_{t+1} - \mathbf{x}_* \rangle \\ = \langle \nabla f(\mathbf{x}_{t+1}) - \nabla f(\mathbf{y}_{t+1}), \mathbf{z}_t - \mathbf{y}_{t+1} \rangle + \langle \nabla f(\mathbf{y}_{t+1}), \mathbf{z}_t - \mathbf{x}_* \rangle \\ \stackrel{(16)}{=} \frac{\beta_{t+1}}{1 + \beta_{t+1}} \langle \nabla f(\mathbf{x}_{t+1}) - \nabla f(\mathbf{y}_{t+1}), \mathbf{y}_{t+1} - \mathbf{x}_{t+1} \rangle + \langle \nabla f(\mathbf{y}_{t+1}), \mathbf{z}_t - \mathbf{x}_* \rangle, \end{aligned} \quad (17)$$

678
679
680

where the third and the fifth lines have applied the convexity of f . Now, because of the convexity of f , observe that for any $a, b \in \mathbb{R}^d$,

681
682

$$\begin{aligned} f(a) &\geq f(b) + \langle \nabla f(b), a - b \rangle \\ f(b) &\geq f(a) + \langle \nabla f(a), b - a \rangle. \end{aligned}$$

683
684

Summing together the two above inequalities gives

685
686
687

$$\langle \nabla f(a) - \nabla f(b), b - a \rangle \leq 0$$

and thus the first term of (17) is negative. This then completes the proof of the lemma. \square

688

689
690

Lemma A.2. Let $\{\mathbf{x}_t, \mathbf{y}_t, \mathbf{z}_t\}$ be generated from (1), (2), (3). Suppose that

691
692

$$c_t = \frac{\gamma_t}{\sum_{i=0}^t \gamma_i}. \quad (18)$$

693
694

Initializing $\mathbf{z}_{-1} = \mathbf{x}_0$, we then have

695
696
697

$$\sum_{t=0}^T \gamma_t (f(\mathbf{x}_T) - f(\mathbf{x}_*)) \leq \gamma_0 (f(\mathbf{x}_0) - f(\mathbf{x}_*)) + \sum_{t=0}^T \gamma_t \langle \nabla f(\mathbf{y}_t), \mathbf{z}_{t-1} - \mathbf{x}_* \rangle. \quad (19)$$

698
699
700

Proof. Applying Lemma A.1 and multiplying (14) by γ_{t+1} ,

701

$$\frac{\gamma_{t+1}}{c_{t+1}} f(\mathbf{x}_{t+1}) - \gamma_{t+1} \left(\frac{1}{c_{t+1}} - 1 \right) f(\mathbf{x}_t) - \gamma_{t+1} f(\mathbf{x}_*) \leq \gamma_{t+1} \langle \nabla f(\mathbf{y}_{t+1}), \mathbf{z}_t - \mathbf{x}_* \rangle. \quad (20)$$

702 Summing of the left-hand side of (20) from $t = 0$ to $T - 1$ gives
 703

$$\begin{aligned}
 704 \quad & \sum_{t=0}^{T-1} \left(\frac{\gamma_{t+1}}{c_{t+1}} f(\mathbf{x}_{t+1}) - \gamma_{t+1} \left(\frac{1}{c_{t+1}} - 1 \right) f(\mathbf{x}_t) - \gamma_{t+1} f(\mathbf{x}_*) \right) \\
 705 \quad & = \frac{\gamma_T}{c_T} f(\mathbf{x}_T) - \gamma_1 \left(\frac{1}{c_1} - 1 \right) f(\mathbf{x}_0) - \sum_{t=1}^T \gamma_t f(\mathbf{x}_*) + \sum_{t=1}^{T-1} \left(\frac{\gamma_t}{c_t} - \gamma_{t+1} \left(\frac{1}{c_{t+1}} - 1 \right) \right) f(\mathbf{x}_t).
 706 \quad & \tag{21}
 707 \\
 708 \quad &
 709 \\
 710 \quad &
 711
 \end{aligned}$$

712 Using (18) we have that the right most term is zero since
 713

$$\begin{aligned}
 714 \quad & \frac{\gamma_t}{c_t} - \gamma_{t+1} \left(\frac{1}{c_{t+1}} - 1 \right) = \sum_{i=0}^t \gamma_i - \left(\sum_{i=0}^{t+1} \gamma_i - \gamma_{t+1} \right) = 0.
 715 \quad &
 716
 \end{aligned}$$

717 We chose the c_t coefficients given in (18) so that the above would be zero. Indeed, instead of
 718 plugging in (18), if we set the above to zero, and unroll the recurrence in c_t we get:
 719

$$\begin{aligned}
 720 \quad & \frac{\gamma_{t+1}}{c_{t+1}} = \gamma_{t+1} + \frac{\gamma_t}{c_t} \\
 721 \quad & = \gamma_{t+1} + \gamma_t + \frac{\gamma_{t-1}}{c_{t-1}} \\
 722 \quad & = \dots \\
 723 \quad & = \sum_{i=1}^{t+1} \gamma_i + \frac{\gamma_0}{c_0},
 724 \quad &
 725
 \end{aligned}$$

726 which gives

$$c_{t+1} = \frac{\gamma_{t+1}}{\sum_{i=0}^{t+1} \gamma_i}$$

727 where we have chosen $c_0 = 1$. Thus we arrive at the same recurrence. Similarly,
 728

$$\gamma_1 \left(\frac{1}{c_1} - 1 \right) = \frac{\gamma_0}{c_0} = \gamma_0$$

729 and

$$\frac{\gamma_T}{c_T} = \sum_{i=0}^T \gamma_i.$$

730 Consequently (21) can be written as
 731

$$\begin{aligned}
 732 \quad & \sum_{t=0}^{T-1} \frac{\gamma_{t+1}}{c_{t+1}} f(\mathbf{x}_{t+1}) - \gamma_{t+1} \left(\frac{1}{c_{t+1}} - 1 \right) f(\mathbf{x}_t) - \gamma_{t+1} f(\mathbf{x}_*) \\
 733 \quad & = \sum_{t=0}^T \gamma_t f(\mathbf{x}_T) - \gamma_0 f(\mathbf{x}_0) - \sum_{t=1}^T \gamma_t f(\mathbf{x}_*) \\
 734 \quad & = \sum_{t=0}^T \gamma_t (f(\mathbf{x}_T) - f(\mathbf{x}_*)) - \gamma_0 (f(\mathbf{x}_0) - f(\mathbf{x}_*)).
 735 \quad & \tag{22}
 736 \\
 737 \quad &
 738
 \end{aligned}$$

739 Putting this back to (20), we can write
 740

$$\begin{aligned}
 741 \quad & \sum_{t=1}^T \gamma_t (f(\mathbf{x}_T) - f(\mathbf{x}_*)) \leq \gamma_0 (f(\mathbf{x}_0) - f(\mathbf{x}_*)) + \sum_{t=0}^{T-1} \gamma_{t+1} \langle \nabla f(\mathbf{y}_{t+1}), \mathbf{z}_t - \mathbf{x}_* \rangle \\
 742 \quad & = \gamma_0 (f(\mathbf{x}_0) - f(\mathbf{x}_*)) + \sum_{t=1}^T \gamma_t \langle \nabla f(\mathbf{y}_t), \mathbf{z}_{t-1} - \mathbf{x}_* \rangle.
 743 \quad &
 744 \\
 745 \quad &
 746
 \end{aligned}$$

747 Because of the convexity of f , we know that
 748

$$\langle \nabla f(\mathbf{x}_0), \mathbf{x}_0 - \mathbf{x}_* \rangle \geq 0.$$

756 Also because we initialize $\mathbf{z}_{-1} = \mathbf{x}_0$, we have

$$757 \quad \langle \nabla f(\mathbf{y}_0), \mathbf{z}_{-1} - \mathbf{x}_* \rangle \geq 0.$$

759 Therefore, with $\gamma_0 \geq 0$, we obtain

$$760 \quad \sum_{t=1}^T \gamma_t (f(\mathbf{x}_T) - f(\mathbf{x}_*)) \leq \gamma_0 (f(\mathbf{x}_0) - f(\mathbf{x}_*)) + \sum_{t=0}^T \gamma_t \langle \nabla f(\mathbf{y}_t), \mathbf{z}_{t-1} - \mathbf{x}_* \rangle.$$

□

765 A.2 PROOF OF THEOREM 2.1

766 **Theorem 2.1.** Let $f: \mathbb{R}^d \rightarrow \mathbb{R}$ be convex and G -Lipschitz continuous. Let $\{\mathbf{x}_t, \mathbf{y}_t, \mathbf{z}_t\}$ be generated from (1), (2), (3). Suppose that

$$767 \quad c_t = \frac{\gamma_t}{\sum_{i=0}^t \gamma_i} \quad (6)$$

771 for $t = 1, \dots, T$. Initializing $\mathbf{z}_{-1} = \mathbf{x}_0$, we then have

$$772 \quad \mathbb{E}[f(\mathbf{x}_T) - f(\mathbf{x}_*)] \leq \frac{\frac{1}{2}\|\mathbf{x}_0 - \mathbf{x}_*\|^2 + \gamma_0(f(\mathbf{x}_0) - f(\mathbf{x}_*))}{\sum_{t=0}^T \gamma_t} + \sum_{t=0}^T \frac{\frac{1}{2}\gamma_t^2 G^2}{\sum_{t=0}^T \gamma_t}. \quad (7)$$

776 *Proof.* Having Lemma A.2 established, it remains to bound the last term of (19). Write $\mathbf{g}_t =$
777 $\nabla f(\mathbf{y}_t, \zeta_t)$. Using the updating rule (2), we see that, for $t = 0, 1, \dots, T-1$,

$$778 \quad \begin{aligned} \|\mathbf{z}_t - \mathbf{x}_*\|^2 &= \|\mathbf{z}_{t-1} - \gamma_t \mathbf{g}_t - \mathbf{x}_*\|^2 \\ 779 &= \|\mathbf{z}_{t-1} - \mathbf{x}_*\|^2 - 2\gamma_t \langle \mathbf{g}_t, \mathbf{z}_{t-1} - \mathbf{x}_* \rangle + \gamma_t^2 \|\mathbf{g}_t\|^2. \end{aligned}$$

781 Rearranging terms, we have

$$782 \quad \langle \mathbf{g}_t, \mathbf{z}_{t-1} - \mathbf{x}_* \rangle = \frac{1}{2\gamma_t} \|\mathbf{z}_{t-1} - \mathbf{x}_*\|^2 - \frac{1}{2\gamma_t} \|\mathbf{z}_t - \mathbf{x}_*\|^2 + \frac{\gamma_t}{2} \|\mathbf{g}_t\|^2. \quad (23)$$

785 Taking expectation conditioned on \mathbf{z}_{t-1} , and noting that $\mathbb{E}_{t-1}[\mathbf{g}_t] = \nabla f(\mathbf{y}_t)$ gives

$$786 \quad \langle \nabla f(\mathbf{y}_t), \mathbf{z}_{t-1} - \mathbf{x}_* \rangle = \frac{1}{2\gamma_t} \|\mathbf{z}_{t-1} - \mathbf{x}_*\|^2 - \frac{1}{2\gamma_t} \mathbb{E}_{t-1}[\|\mathbf{z}_t - \mathbf{x}_*\|^2] + \frac{\gamma_t}{2} \mathbb{E}_{t-1}[\|\mathbf{g}_t\|^2]. \quad (24)$$

788 Taking full expectation and using the law of total expectation gives

$$790 \quad \mathbb{E} \langle \nabla f(\mathbf{y}_t), \mathbf{z}_{t-1} - \mathbf{x}_* \rangle = \frac{1}{2\gamma_t} \mathbb{E} \|\mathbf{z}_{t-1} - \mathbf{x}_*\|^2 - \frac{1}{2\gamma_t} \mathbb{E} \|\mathbf{z}_t - \mathbf{x}_*\|^2 + \frac{\gamma_t}{2} \mathbb{E} \|\mathbf{g}_t\|^2.$$

792 Multiplying by γ_t and summing it up from $t = 0$ to T , we have

$$793 \quad \begin{aligned} \sum_{t=0}^T \gamma_t \mathbb{E} \langle \nabla f(\mathbf{y}_t), \mathbf{z}_{t-1} - \mathbf{x}_* \rangle &= \sum_{t=0}^T \left(\frac{1}{2} \mathbb{E} \|\mathbf{z}_{t-1} - \mathbf{x}_*\|^2 - \frac{1}{2} \mathbb{E} \|\mathbf{z}_t - \mathbf{x}_*\|^2 + \frac{\gamma_t^2}{2} \mathbb{E} \|\mathbf{g}_t\|^2 \right) \\ 794 &= \frac{1}{2} \|\mathbf{z}_{-1} - \mathbf{x}_*\|^2 - \frac{1}{2} \mathbb{E} \|\mathbf{z}_T - \mathbf{x}_*\|^2 + \sum_{t=0}^T \frac{\gamma_t^2}{2} \mathbb{E} \|\mathbf{g}_t\|^2 \\ 795 &= \frac{1}{2} \|\mathbf{x}_0 - \mathbf{x}_*\|^2 - \frac{1}{2} \mathbb{E} \|\mathbf{z}_T - \mathbf{x}_*\|^2 + \sum_{t=0}^T \frac{\gamma_t^2}{2} \mathbb{E} \|\mathbf{g}_t\|^2. \end{aligned} \quad (25)$$

802 Dropping the negative $-\frac{1}{2} \mathbb{E} \|\mathbf{z}_T - \mathbf{x}_*\|^2$ term, and using the above in (19) we have that

$$804 \quad \begin{aligned} \sum_{t=0}^T \gamma_t \mathbb{E} [f(\mathbf{x}_T) - f(\mathbf{x}_*)] &\leq \gamma_0 (f(\mathbf{x}_0) - f(\mathbf{x}_*)) + \sum_{t=0}^T \gamma_t \mathbb{E} \langle \nabla f(\mathbf{y}_t), \mathbf{z}_{t-1} - \mathbf{x}_* \rangle \\ 805 &\leq \gamma_0 (f(\mathbf{x}_0) - f(\mathbf{x}_*)) + \frac{1}{2} \|\mathbf{x}_0 - \mathbf{x}_*\|^2 + \sum_{t=0}^T \frac{\gamma_t^2}{2} \mathbb{E} \|\mathbf{g}_t\|^2. \end{aligned}$$

809 Finally dividing through by $\sum_{t=0}^T \gamma_t$ gives the result. □

810 A.3 PROOF OF LEMMA 2.2

811 **Lemma 2.2.** Let $0 \leq T_w \leq T_c \leq T$ and $\gamma > 0$. Suppose that $\{\eta_t\}_{t=0}^T$ follows the wsd schedule
 812 given in (8). We can determine $\{c_t\}_{t=0}^T$ by

$$814 \quad c_t = \begin{cases} \frac{2}{t+2}, & \text{if } 0 \leq t \leq T_w, \\ 815 \quad \frac{2}{2t-T_w+2}, & \text{if } T_w < t \leq T_c, \\ 816 \quad \frac{2(T-t+1)}{(T-T_c+1)(2T_c-T_w+2)+(2T-T_c-t+1)(t-T_c)}, & \text{if } T_c < t \leq T. \end{cases} \quad (9)$$

818 *Proof.* Recall from (6) is given by

$$821 \quad c_t = \frac{\eta_t}{\sum_{i=0}^t \eta_i}. \quad (26)$$

824 for some scheduler $\{\eta_t\}_{t=0}^T$. Now, we are ready to obtain $\{c_t\}_{t=0}^T$ by substituting the wsd scheduler
 825 $\{\eta_t\}_{t=0}^T$ and applying the arithmetic formula. Specifically, for $0 \leq t \leq T_w$,

$$827 \quad c_t = \frac{\frac{t+1}{T_w+1}}{\frac{\sum_{i=0}^t (i+1)}{T_w+1}} = \frac{t+1}{\frac{(t+1)(t+2)}{2}} = \frac{2}{t+2}.$$

830 Since

$$832 \quad \sum_{i=0}^{T_w} \eta_i = \sum_{i=0}^{T_w} \frac{t+1}{T_w+1} = \frac{\frac{(T_w+1)(T_w+2)}{2}}{T_w+1} = \frac{T_w+2}{2}, \quad (27)$$

835 we obtain, for $T_w < t \leq T_c$,

$$837 \quad c_t = \frac{1}{\sum_{i=0}^{T_w} \eta_i + \sum_{i=T_w+1}^t \eta_i} = \frac{1}{\frac{T_w+2}{2} + (t - T_w)} = \frac{2}{2t - T_w + 2}.$$

839 Applying (27) again and using

$$841 \quad \sum_{i=T_w+1}^{T_c} \eta_i = T_c - T_w,$$

844 we also have, for $T_c < t \leq T$,

$$846 \quad c_t = \frac{\frac{T-t+1}{T-T_c+1}}{\sum_{i=0}^{T_w} \eta_i + \sum_{i=T_w+1}^{T_c} \eta_i + \sum_{i=T_c+1}^t \frac{T-i+1}{T-T_c+1}} \\ 847 = \frac{\frac{T-t+1}{T-T_c+1}}{\frac{T_w+2}{2} + (T_c - T_w) + \frac{(2T-T_c-t+1)(t-T_c)}{2(T-T_c+1)}} \\ 848 = \frac{2(T-t+1)}{(T-T_c+1)(2T_c-T_w+2) + (2T-T_c-t+1)(t-T_c)}.$$

855 \square

856 A.4 PROOF OF COROLLARY 2.3

858 **Corollary 2.3.** Let $D = \|\mathbf{x}_0 - \mathbf{x}_\star\|$. Using the wsd parameters (c_t, η_t) given in (9) and (8), with
 859 a base learning rate of $\gamma = \frac{D}{G\sqrt{\sum_{t=0}^T \eta_t^2}}$, we have the convergence

$$862 \quad \mathbb{E}[f(\mathbf{x}_T) - \inf f] \leq \frac{2\eta_0(f(\mathbf{x}_0) - f(\mathbf{x}_\star))}{T + T_c - T_w + 2} + \frac{2\sqrt{\frac{2}{3}}DG}{\sqrt{T + T_c - T_w + 2}} \simeq \mathcal{O}\left(\frac{DG}{\sqrt{T}}\right). \quad (10)$$

864 *Proof.* Using the arithmetic sum formula, we can write
 865

$$\begin{aligned}
 866 \quad \sum_{t=0}^{T_w-1} \eta_t &= \frac{\sum_{t=0}^{T_w-1} (t+1)}{T_w + 1} = \frac{T_w + \sum_{t=0}^{T_w-1} t}{T_w + 1} = \frac{T_w + \frac{T_w(T_w-1)}{2}}{T_w + 1} = \frac{T_w}{2}; \\
 867 \\
 868 \quad \sum_{t=T_w}^{T_c-1} \eta_t &= T_c - 1 - T_w + 1 = T_c - T_w \\
 869 \\
 870 \quad \sum_{t=T_c}^T \eta_t &= \sum_{t=T_c}^T \frac{T-t+1}{T-T_c+1} = \frac{(T+1)(T-T_c+1)}{T-T_c+1} - \frac{\sum_{t=T_c}^T t}{T-T_c+1} \\
 871 \\
 872 \quad &= T+1 - \frac{(T_c+T)(T-T_c+1)}{2(T-T_c+1)} = T+1 - \frac{T_c+T}{2}. \tag{28}
 \end{aligned}$$

873 Combining, we have
 874

$$\sum_{t=0}^T \eta_t = \frac{T_w}{2} + T_c - T_w + T + 1 - \frac{T_c+T}{2} = \frac{T+T_c-T_w+2}{2}. \tag{29}$$

875 Also, using the fact that
 876

$$\sum_{k=1}^n k^2 = \frac{n(n+1)(2n+1)}{6}, \tag{30}$$

877 we can compute
 878

$$\begin{aligned}
 879 \quad \sum_{t=0}^{T_w-1} \eta_t^2 &= \sum_{t=0}^{T_w-1} \frac{(t+1)^2}{(T_w+1)^2} = \frac{\sum_{t=0}^{T_w-1} t^2 + 2 \sum_{t=0}^{T_w-1} t + T_w}{(T_w+1)^2} \\
 880 \\
 881 \quad &= \frac{\frac{T_w(T_w-1)(2T_w-1)}{6} + 2 \frac{T_w(T_w-1)}{2} + T_w}{(T_w+1)^2} = \frac{T_w}{T_w+1} \cdot \frac{\frac{(T_w-1)(2T_w-1)}{6} + T_w}{T_w+1} \\
 882 \\
 883 \quad &\leq \frac{2T_w^2 + 3T_w + 1}{6(T_w+1)} = \frac{(2T_w+1)(T_w+1)}{6(T_w+1)} = \frac{2T_w+1}{6}; \\
 884 \\
 885 \quad \sum_{t=T_w}^{T_c-1} \eta_t^2 &= T_c - 1 - T_w + 1 = T_c - T_w; \\
 886 \\
 887 \quad \sum_{t=T_c}^T \eta_t^2 &= \frac{\sum_{t=T_c}^T (T-t+1)^2}{(T-T_c+1)^2} = \frac{\sum_{t=1}^{T-T_c+1} t^2}{(T-T_c+1)^2} \\
 888 \\
 889 \quad &= \frac{(T-T_c+1)(T-T_c+2)(2T-2T_c+3)}{6(T-T_c+1)^2} \\
 890 \\
 891 \quad &= \frac{(T-T_c+2)(2T-2T_c+3)}{6(T-T_c+1)} \\
 892 \\
 893 \quad &= \frac{(T-T_c+1)(2T-2T_c+3) + (2T-2T_c+3)}{6(T-T_c+1)} \\
 894 \\
 895 \quad &= \frac{1}{6} \left(2T-2T_c+3 + \frac{2T-2T_c+3}{T-T_c+1} \right) \\
 896 \\
 897 \quad &= \frac{1}{6} \left(2T-2T_c+3 + \frac{2(T-T_c+1)+1}{T-T_c+1} \right) \\
 898 \\
 899 \quad &= \frac{1}{6} \left(2T-2T_c+3 + 2 + \frac{1}{T-T_c+1} \right) \\
 900 \\
 901 \quad &\leq \frac{1}{6} (2T-2T_c+3+2+1) = \frac{T}{3} - \frac{T_c}{3} + 1. \tag{31}
 \end{aligned}$$

918 Combining, we have
 919

$$\begin{aligned} 920 \quad \sum_{t=0}^T \eta_t^2 &= \frac{2T_w + 1}{6} + T_c - T_w + \frac{T}{3} - \frac{T_c}{3} + 1 = \frac{T + 2T_c - 2T_w}{3} + \frac{7}{6} \\ 921 \\ 922 \quad &\leq \frac{2}{3}(T + T_c - T_w + 2). \end{aligned} \quad (32)$$

923 Applying the results to Theorem 2.1 then establishes the corollary. \square
 925

926 A.5 COMMENTS ON THE WEIGHTS c_t IN DEFAZIO ET AL. (2024)

928 Defazio et al. (2024) suggested the convergence rate of $\mathcal{O}(1/\sqrt{T})$ as long as the averaging parameter
 929 is in the form of $c_t = w_t / \sum_{i=1}^t w_i$ for any $w_t \in [0, 1]$ for $t = 1, \dots, T$. While the condition might
 930 look slightly more general than our proposed c_t in (6), we show that, after applying the standard
 931 online convex optimization technique to (Defazio et al., 2024, Theorem 2), the averaging parameter
 932 c_t has to satisfy (6) in order to get a valid convergence bound.
 933

934 To show this, let us first recall (Defazio et al., 2024, Theorem 2).

935 **Theorem A.3** (Defazio et al. (2024, Theorem 2)). Let $f: \mathbb{R}^d \rightarrow \mathbb{R}$ be a convex function and
 936 ζ_1, \dots, ζ_T be an iid sequence. Let β_1, \dots, β_T and w_1, \dots, w_T be numbers in $[0, 1]$ that are
 937 independent of ζ_1, \dots, ζ_T . Consider the iterates $(\mathbf{x}_t, \mathbf{y}_t, \mathbf{z}_t)$ generated by the following:
 938

$$\mathbf{x}_t = \underbrace{\left(1 - \frac{w_t}{\sum_{i=1}^t w_i}\right)}_{=:1-c_t} \mathbf{x}_{t-1} + \underbrace{\frac{w_t}{\sum_{i=1}^t w_i}}_{=:c_t} \mathbf{z}_t \quad (33)$$

$$\mathbf{y}_t = \beta_t \mathbf{x}_t + (1 - \beta_t) \mathbf{z}_t \quad (34)$$

$$\mathbf{z}_{t+1} = \mathbf{z}_t - \gamma_t \mathbf{g}_t, \quad \mathbf{g}_t := \nabla f(\mathbf{y}_t, \zeta_t). \quad (35)$$

945 Then, we have that
 946

$$\mathbb{E}[f(\mathbf{x}_T) - f(\mathbf{x}_*)] \leq \frac{\mathbb{E}\left[\sum_{t=1}^T w_t \langle \mathbf{g}_t, \mathbf{z}_t - \mathbf{x}_* \rangle\right]}{\sum_{i=1}^T w_i}.$$

951 Before going into the proof, we would like to give a heads-up that the indices of \mathbf{z}_t in Defazio et al.
 952 (2024) (as shown in (33)–(35)) is slightly different from our paper (given in (1)–(3)). In this part, we
 953 will stick to the updating rule (33)–(35) to derive the condition on c_t based on the results in Defazio
 954 et al. (2024, Theorem 2).

955 From the updating rule (35), we know that
 956

$$\begin{aligned} 957 \quad \|\mathbf{z}_{t+1} - \mathbf{x}_*\|^2 &= \|\mathbf{z}_t - \gamma_t \mathbf{g}_t - \mathbf{x}_*\|^2 \\ 958 \quad &= \|\mathbf{z}_t - \mathbf{x}_*\|^2 - 2\gamma_t \langle \mathbf{g}_t, \mathbf{z}_t - \mathbf{x}_* \rangle + \gamma_t^2 \|\mathbf{g}_t\|^2, \end{aligned}$$

959 which implies
 960

$$\langle \mathbf{g}_t, \mathbf{z}_t - \mathbf{x}_* \rangle = \frac{1}{2\gamma_t} \|\mathbf{z}_t - \mathbf{x}_*\|^2 - \frac{1}{2\gamma_t} \|\mathbf{z}_{t+1} - \mathbf{x}_*\|^2 + \frac{\gamma_t}{2} \|\mathbf{g}_t\|^2.$$

963 Therefore, multiplying by w_t , taking expectation, and summing it up from $t = 1$ to T would yield
 964

$$\begin{aligned} 965 \quad \mathbb{E}\left[\sum_{t=1}^T w_t \langle \mathbf{g}_t, \mathbf{z}_t - \mathbf{x}_* \rangle\right] &= \mathbb{E}\left[\sum_{t=1}^T \left(\frac{w_t}{2\gamma_t} \|\mathbf{z}_t - \mathbf{x}_*\|^2 - \frac{w_t}{2\gamma_t} \|\mathbf{z}_{t+1} - \mathbf{x}_*\|^2 + \frac{w_t \gamma_t}{2} \|\mathbf{g}_t\|^2\right)\right] \\ 966 \\ 967 \quad &\leq \frac{w_1}{2\gamma_1} \|\mathbf{z}_1 - \mathbf{x}_*\|^2 + \sum_{t=2}^T \mathbb{E}\left[\left(\frac{w_t}{2\gamma_t} - \frac{w_{t-1}}{2\gamma_{t-1}}\right) \|\mathbf{z}_t - \mathbf{x}_*\|^2\right] + \sum_{t=1}^T \frac{w_t \gamma_t}{2} \mathbb{E}[\|\mathbf{g}_t\|^2]. \end{aligned}$$

970 Therefore, to obtain a last-iterate convergence bound, we want

$$\frac{w_t}{\gamma_t} = \frac{w_{t-1}}{\gamma_{t-1}} \quad (36)$$

972 for $t = 2, \dots, T$ such that the second term gets canceled out. Unrolling,

$$\begin{aligned}
 973 \quad w_t &= w_{t-1} \cdot \frac{\gamma_t}{\gamma_{t-1}} \\
 974 \quad &= w_{t-2} \cdot \frac{\gamma_{t-1}}{\gamma_{t-2}} \cdot \frac{\gamma_t}{\gamma_{t-1}} = w_{t-2} \cdot \frac{\gamma_t}{\gamma_{t-2}} \\
 975 \quad &= \dots \\
 976 \quad &= \gamma_t \cdot \frac{w_1}{\gamma_1}.
 \end{aligned} \tag{37}$$

981 Therefore, the condition on c_t is given by

$$982 \quad c_t = \frac{w_t}{\sum_{i=1}^t w_i} = \frac{\gamma_t \cdot \frac{w_1}{\gamma_1}}{\sum_{i=1}^t \gamma_i \cdot \frac{w_1}{\gamma_1}} = \frac{\gamma_t}{\sum_{i=1}^t \gamma_i},$$

984 which is the same as our condition (6). Moreover, using (37) again, we have that

$$985 \quad \sum_{i=1}^T w_i = \frac{w_1}{\gamma_1} \sum_{i=1}^T \gamma_i,$$

988 and hence we have the convergence

$$\begin{aligned}
 989 \quad \mathbb{E}[f(\mathbf{x}_T) - f(\mathbf{x}_*)] &\leq \frac{\mathbb{E}\left[\sum_{t=1}^T w_t \langle \mathbf{g}_t, \mathbf{z}_t - \mathbf{x}_* \rangle\right]}{\sum_{i=1}^T w_i} \\
 990 \quad &\leq \frac{\frac{w_1}{2\gamma_1} \|\mathbf{z}_1 - \mathbf{x}_*\|^2 + \sum_{t=1}^T \frac{w_t \gamma_t}{2} \mathbb{E}[\|\mathbf{g}_t\|^2]}{\sum_{i=1}^T w_i} \\
 991 \quad &= \frac{\frac{1}{2} \|\mathbf{z}_1 - \mathbf{x}_*\|^2 + \frac{1}{2} \sum_{t=1}^T \gamma_t^2 \mathbb{E}[\|\mathbf{g}_t\|^2]}{\sum_{t=1}^T \gamma_t},
 \end{aligned}$$

998 which achieves the same bound as in Theorem 2.1.

1000 B PROOFS FOR POLYAK STEPSIZE

1001 B.1 DERIVATION OF THE SCHEDULED LEARNING RATE

1004 Starting by expanding the squares of the distance to the solution \mathbf{x}_* we have

$$1005 \quad \|\mathbf{z}_t - \mathbf{x}_*\|^2 = \|\mathbf{z}_{t-1} - \mathbf{x}_*\|^2 - 2\gamma_t \langle \nabla f(\mathbf{y}_t, \zeta_t), \mathbf{z}_{t-1} - \mathbf{x}_* \rangle + \gamma_t^2 \|\nabla f(\mathbf{y}_t, \zeta_t)\|^2. \tag{38}$$

1006 We could now minimize the right hand side in γ_t , but then the solution would depend directly on the
1007 unknown \mathbf{x}_* . So before minimizing in γ_t , we need to upper bound the right hand side with terms we
1008 do know.

1009 To simplify notation, let us consider $\beta_t \equiv \beta$ for all t . Re-arranging (1) gives

$$1011 \quad \mathbf{z}_{t-1} = \frac{1}{1-\beta} \mathbf{y}_t - \left(\frac{1}{1-\beta} - 1 \right) \mathbf{x}_t = \mathbf{y}_t - \frac{\beta}{1-\beta} (\mathbf{x}_t - \mathbf{y}_t) \tag{39}$$

1013 Now the above in (38) gives

$$\begin{aligned}
 1014 \quad \|\mathbf{z}_t - \mathbf{x}_*\|^2 &= \|\mathbf{z}_{t-1} - \mathbf{x}_*\|^2 + \gamma_t^2 \|\nabla f(\mathbf{y}_t, \zeta_t)\|^2 \\
 1015 \quad &\quad - 2\gamma_t \langle \nabla f(\mathbf{y}_t, \zeta_t), \mathbf{y}_t - \mathbf{x}_* \rangle + 2\gamma_t \frac{\beta}{1-\beta} \langle \nabla f(\mathbf{y}_t, \zeta_t), \mathbf{x}_t - \mathbf{y}_t \rangle.
 \end{aligned}$$

1018 Now using convexity we have that

$$1019 \quad - \langle \nabla f(\mathbf{y}_t, \zeta_t), \mathbf{y}_t - \mathbf{x}_* \rangle \leq f_{\zeta_t}(\mathbf{x}_*) - f_{\zeta_t}(\mathbf{y}_t)$$

1020 and using that $\mathbf{y}_t - \mathbf{x}_t = (1-\beta)(\mathbf{z}_{t-1} - \mathbf{x}_*)$ gives

$$\begin{aligned}
 1021 \quad \|\mathbf{z}_t - \mathbf{x}_*\|^2 &\leq \|\mathbf{z}_{t-1} - \mathbf{x}_*\|^2 + \gamma_t^2 \|\nabla f(\mathbf{y}_t, \zeta_t)\|^2 \\
 1022 \quad &\quad - 2\gamma_t ((f_{\zeta_t}(\mathbf{y}_t) - f_{\zeta_t}(\mathbf{x}_*)) - 2\gamma_t \beta \langle \nabla f(\mathbf{y}_t, \zeta_t), \mathbf{z}_{t-1} - \mathbf{x}_t \rangle).
 \end{aligned} \tag{40}$$

1024 Minimizing over $\gamma_t \geq 0$ gives

$$1025 \quad \gamma_t = \frac{(f_{\zeta_t}(\mathbf{y}_t) - f_{\zeta_t}(\mathbf{x}_*)) + \beta \langle \nabla f(\mathbf{y}_t, \zeta_t), \mathbf{z}_{t-1} - \mathbf{x}_t \rangle_+}{\|\nabla f(\mathbf{y}_t, \zeta_t)\|^2}. \tag{41}$$

1026 B.2 AUXILIARY LEMMAS
10271028 **Lemma B.1** (Extended Titu's Lemma). For any random variable X and positive-valued random
1029 variable Y , it holds

1030
$$\mathbb{E} \left[\frac{(X)_+^2}{Y} \right] \geq \frac{(\mathbb{E}[X])_+^2}{\mathbb{E}[Y]}. \quad (42)$$

1031

1032 In addition, for any numbers a_0, \dots, a_k and positive numbers b_0, \dots, b_k , we have

1033
$$\sum_{t=0}^k \frac{(a_t)_+^2}{b_t} \geq \frac{\left(\sum_{t=0}^k a_t \right)_+^2}{\sum_{t=0}^k b_t}. \quad (43)$$

1034
1035
1036

1037 **Lemma B.2.** If f_ζ is convex for every ζ , and we use the learning rate (41) we have that

1038
$$\|z_t - x_\star\|^2 \leq \|z_{t-1} - x_\star\|^2 - \frac{(f_{\zeta_t}(y_t) - f_{\zeta_t}(x_\star) + \beta \langle \nabla f(y_t, \zeta_t), z_{t-1} - x_t \rangle)_+^2}{\|\nabla f(y_t, \zeta_t)\|^2}. \quad (44)$$

1039
1040
1041

1042 As a consequence we also have that $\|z_t - x_\star\|$, $\|x_t - x_\star\|$ and $\|y_t - x_\star\|$ are less than $\|x_0 - x_\star\|$.
1043 Furthermore, taking expectation we have that

1044
$$\mathbb{E} [\|z_t - x_\star\|^2] \leq \mathbb{E} [\|z_{t-1} - x_\star\|^2] - \frac{(\mathbb{E}[f(y_t) - f(x_\star) + \beta \langle \nabla f(y_t), z_{t-1} - x_t \rangle])_+^2}{\mathbb{E} [\|\nabla f(y_t, \zeta_t)\|^2]}. \quad (45)$$

1045
1046
1047
1048
1049

1050 *Proof.* Inserting (41) into (40) gives the first result, which also shows that $\|z_t - x_\star\| \leq \|z_0 - x_\star\| =$
1051 $\|x_0 - x_\star\|$. Since x_{t+1} is a convex combination of x_t and z_t , we have that

1052
$$\|x_{t+1} - x_\star\| \leq (1 - c_{t+1})\|x_t - x_\star\| + c_{t+1}\|z_t - x_\star\|$$

1053

1054 from which we can use induction to show $\|x_t - x_\star\| \leq \|x_0 - x_\star\|$. Furthermore, since y_t is a
1055 convex combination of z_{t-1} and x_t , it also follows by induction that $\|y_t - x_\star\| \leq \|x_0 - x_\star\|$.1056 Taking conditional expectation over (44) given x_t and z_{t-1} and using Lemma B.1 gives

1057
$$\mathbb{E}_t [\|z_t - x_\star\|^2] \leq \|z_{t-1} - x_\star\|^2 - \frac{(f(y_t) - f(x_\star) + \beta \langle \nabla f(y_t), z_{t-1} - x_t \rangle)_+^2}{\mathbb{E}_t [\|\nabla f(y_t, \zeta_t)\|^2]}. \quad (46)$$

1058
1059

1060 Finally, taking total expectation over (46), and using the law of total expectation and Lemma B.1
1061 again, yields (45). \square

1062 Next we develop the Bregman viewpoint of this method.

1063 **Lemma B.3.** Let $\lambda = \frac{\beta}{1-\beta}$. It follows that

1064
$$\begin{aligned} f(y_t) - f(x_\star) + \beta \langle \nabla f(y_t), z_{t-1} - x_t \rangle &= (1 + \lambda)(f(y_t) - f(x_\star)) \\ &\quad - \lambda(f(x_t) - f(x_\star)) \\ &\quad + \lambda B_f(x_t, y_t), \end{aligned} \quad (47)$$

1065
1066
1067
1068
1069

1070 where $B_f(x_t, y_t)$ is the Bregman divergence of f that is

1071
$$B_f(x, y) := f(x) - f(y) - \langle \nabla f(y), x - y \rangle.$$

1072
1073

1074 *Proof.* Using $z_{t-1} - x_t = \frac{1}{1-\beta}(y_t - x_t)$ which follows from (1) gives

1075
$$\begin{aligned} f(y_t) - f(x_\star) + \beta \langle \nabla f(y_t), z_{t-1} - x_t \rangle &= f(y_t) - f(x_\star) - \frac{\beta}{1-\beta} \langle \nabla f(y_t), x_t - y_t \rangle \\ &= (1 + \lambda)(f(y_t) - f(x_\star)) - \lambda(f(x_t) - f(x_\star)) \\ &\quad + \lambda(f(x_t) - f(y_t) - \langle \nabla f(y_t), x_t - y_t \rangle). \end{aligned}$$

1076
1077
1078
1079

1080

1081

1082

1083

Lemma B.4. Let $c_t = 1/(t+1)$. Initializing $\mathbf{z}_{-1} = \mathbf{x}_0$, it follows that

$$\begin{aligned} \mathbb{E} [\|\mathbf{z}_t - \mathbf{x}_*\|^2] &\leq \|\mathbf{x}_0 - \mathbf{x}_*\|^2 \\ &\quad - \frac{((t+1)\mathbb{E}[f(\mathbf{x}_t) - f(\mathbf{x}_*)] + \lambda \sum_{k=0}^t \mathbb{E}[B_f(\mathbf{x}_k, \mathbf{y}_k)])_+^2}{\sum_{k=0}^t \mathbb{E}[\|\nabla f(\mathbf{y}_k, \zeta_k)\|^2]}. \end{aligned} \quad (48)$$

1088

1089

1090

Proof. Using (47) in (45) gives

$$\begin{aligned} \mathbb{E} [\|\mathbf{z}_t - \mathbf{x}_*\|^2] &= \mathbb{E} [\|\mathbf{z}_{t-1} - \mathbf{x}_*\|^2] \\ &\quad - \frac{(\mathbb{E}[(1+\lambda)(f(\mathbf{y}_t) - f(\mathbf{x}_*)) - \lambda(f(\mathbf{x}_t) - f(\mathbf{x}_*)) + \lambda B_f(\mathbf{x}_t, \mathbf{y}_t)])_+^2}{\mathbb{E}[\|\nabla f(\mathbf{y}_t, \zeta_t)\|^2]}. \end{aligned} \quad (49)$$

1094

Therefore, unrolling (49) gives

$$\mathbb{E} [\|\mathbf{z}_t - \mathbf{x}_*\|^2] \leq \|\mathbf{z}_{-1} - \mathbf{x}_*\|^2 - \sum_{k=0}^t \frac{(a_k)_+^2}{b_k},$$

1099

1100

1101

where we define $a_k := \mathbb{E}[(1+\lambda)(f(\mathbf{y}_k) - f(\mathbf{x}_*)) - \lambda(f(\mathbf{x}_k) - f(\mathbf{x}_*)) + \lambda B_f(\mathbf{x}_k, \mathbf{y}_k)]$ and $b_k = \mathbb{E}[\|\nabla f(\mathbf{y}_k, \zeta_k)\|^2]$. From Lemma B.1, we know that

$$\sum_{k=0}^t \frac{(a_k)_+^2}{b_k} \geq \frac{(\sum_{k=0}^t a_k)_+^2}{\sum_{k=0}^t b_k}.$$

1105

1106

Therefore, we have that

$$\begin{aligned} \mathbb{E} [\|\mathbf{z}_t - \mathbf{x}_*\|^2] &= \|\mathbf{z}_{-1} - \mathbf{x}_*\|^2 \\ &\quad - \frac{(\sum_{k=0}^t \mathbb{E}[(1+\lambda)(f(\mathbf{y}_k) - f(\mathbf{x}_*)) - \lambda(f(\mathbf{x}_k) - f(\mathbf{x}_*)) + \lambda B_f(\mathbf{x}_k, \mathbf{y}_k)])_+^2}{\sum_{k=0}^t \mathbb{E}[\|\nabla f(\mathbf{y}_k, \zeta_k)\|^2]}. \end{aligned} \quad (50)$$

1112

1113

To finish the proof of convergence, we need to write \mathbf{y}_t as a combination of \mathbf{x}_t and \mathbf{x}_{t-1} so that we can telescope. To this end note that

$$\mathbf{z}_{t-1} = \frac{1}{c_t} \mathbf{x}_t + \left(1 - \frac{1}{c_t}\right) \mathbf{x}_{t-1}.$$

1117

Substituting this into the \mathbf{y}_t update (1) gives

$$\begin{aligned} \mathbf{y}_t &= (1 - \beta) \left(\frac{1}{c_t} \mathbf{x}_t + \left(1 - \frac{1}{c_t}\right) \mathbf{x}_{t-1} \right) + \beta \mathbf{x}_t \\ &= \left((1 - \beta) \left(\frac{1}{c_t} - 1 \right) + 1 \right) \mathbf{x}_t - (1 - \beta) \left(\frac{1}{c_t} - 1 \right) \mathbf{x}_{t-1}. \end{aligned}$$

1123

1124

1125

Let $\rho_t := (1 - \beta) \left(\frac{1}{c_t} - 1 \right)$. Isolating \mathbf{x}_t in the above we have that it can be expressed as a convex combination between \mathbf{y}_t and \mathbf{x}_{t-1} given by

$$\mathbf{x}_t = \frac{1}{1 + \rho_t} \mathbf{y}_t + \frac{\rho_t}{1 + \rho_t} \mathbf{x}_{t-1}. \quad (51)$$

1128

1129

Using the convexity of f we have that

$$f(\mathbf{x}_t) \leq \frac{1}{1 + \rho_t} f(\mathbf{y}_t) + \frac{\rho_t}{1 + \rho_t} f(\mathbf{x}_{t-1}). \quad (52)$$

1132

1133

Re-arranging and isolating $f(\mathbf{y}_t)$ gives

$$f(\mathbf{y}_t) \geq (1 + \rho_t) f(\mathbf{x}_t) - \rho_t f(\mathbf{x}_{t-1}). \quad (53)$$

1134 Using the above we have that

$$\begin{aligned}
 1135 \quad (1 + \lambda)(f(\mathbf{y}_t) - f(\mathbf{x}_*)) - \lambda(f(\mathbf{x}_t) - f(\mathbf{x}_*)) &\geq (1 + \lambda)(1 + \rho_t)(f(\mathbf{x}_t) - f(\mathbf{x}_*)) \\
 1136 \quad &\quad - (1 + \lambda)\rho_t(f(\mathbf{x}_{t-1}) - f(\mathbf{x}_*)) \\
 1137 \quad &\quad - \lambda(f(\mathbf{x}_t) - f(\mathbf{x}_*)) \\
 1138 \quad &\quad = (1 + (1 + \lambda)\rho_t)(f(\mathbf{x}_t) - f(\mathbf{x}_*)) \\
 1139 \quad &\quad - (1 + \lambda)\rho_t(f(\mathbf{x}_{t-1}) - f(\mathbf{x}_*)) \\
 1140 \quad &\quad
 \end{aligned}$$

1141 Substituting back $\rho_t := (1 - \beta) \left(\frac{1}{c_t} - 1 \right)$ and $1 + \lambda = \frac{1}{1 - \beta}$ in the above and using that $c_t =$
 1142 $1/(t + \frac{1}{c_0})$ gives
 1143

$$\begin{aligned}
 1144 \quad (1 + \lambda)(f(\mathbf{y}_t) - f(\mathbf{x}_*)) - \lambda(f(\mathbf{x}_t) - f(\mathbf{x}_*)) \\
 1145 \quad &\geq \left(\frac{1}{c_t} \right) (f(\mathbf{x}_t) - f(\mathbf{x}_*)) - \left(\frac{1}{c_t} - 1 \right) (f(\mathbf{x}_{t-1}) - f(\mathbf{x}_*)) \\
 1146 \quad &= \left(t + \frac{1}{c_0} \right) (f(\mathbf{x}_t) - f(\mathbf{x}_*)) - \left(t - 1 + \frac{1}{c_0} \right) (f(\mathbf{x}_{t-1}) - f(\mathbf{x}_*)).
 \end{aligned}$$

1147 Using the above we have that

$$\begin{aligned}
 1148 \quad &\sum_{k=0}^t ((1 + \lambda)(f(\mathbf{y}_k) - f(\mathbf{x}_*)) - \lambda(f(\mathbf{x}_k) - f(\mathbf{x}_*))) \\
 1149 \quad &\geq f(\mathbf{x}_0) - f(\mathbf{x}_*) + \sum_{k=1}^t \left(\left(k + \frac{1}{c_0} \right) (f(\mathbf{x}_k) - f(\mathbf{x}_*)) - \left(k - 1 + \frac{1}{c_0} \right) (f(\mathbf{x}_{k-1}) - f(\mathbf{x}_*)) \right) \\
 1150 \quad &= f(\mathbf{x}_0) - f(\mathbf{x}_*) + \left(t + \frac{1}{c_0} \right) (f(\mathbf{x}_t) - f(\mathbf{x}_*)) - \frac{1}{c_0} (f(\mathbf{x}_0) - f(\mathbf{x}_*)) \\
 1151 \quad &= (t + 1)(f(\mathbf{x}_t) - f(\mathbf{x}_*)).
 \end{aligned}$$

1152 Inserting this in (50), together with the monotonicity of the positive part and the initialization that
 1153 $\mathbf{z}_{-1} = \mathbf{x}_0$, gives

$$\begin{aligned}
 1154 \quad \mathbb{E} [\|\mathbf{z}_t - \mathbf{x}_*\|^2] &= \|\mathbf{x}_0 - \mathbf{x}_*\|^2 \\
 1155 \quad &\quad - \frac{((t + 1)\mathbb{E}[f(\mathbf{x}_t) - f(\mathbf{x}_*)] + \lambda \sum_{k=0}^t \mathbb{E}[B_f(\mathbf{x}_k, \mathbf{y}_k)])^2_+}{\sum_{k=0}^t \mathbb{E}[\|\nabla f(\mathbf{y}_k, \zeta_k)\|^2]}.
 \end{aligned} \tag{54}$$

□

1169 B.3 PROOF OF THEOREM 3.2

1170 **Theorem 3.2.** Consider the iterates of Algorithm 1 with $c_t = 1/(t + 1)$, $\beta \in [0, 1)$ and $\gamma_{\max} = \infty$. Let $f_\zeta: \mathbb{R}^d \rightarrow \mathbb{R}$ be a convex function for every ζ . Let

$$B := \{\mathbf{x} : \|\mathbf{x} - \mathbf{x}_*\| \leq \|\mathbf{x}_0 - \mathbf{x}_*\|\} \subset \mathbb{R}^d, \tag{11}$$

$$G^2 := \max_{\mathbf{x} \in B} \mathbb{E}_\zeta \|\nabla f(\mathbf{x}, \zeta)\|^2. \tag{12}$$

1171 With the initialization $\mathbf{z}_{-1} = \mathbf{x}_0$, the suboptimality gap of the *last iterate* \mathbf{x}_t converges at a $1/\sqrt{t}$
 1172 rate according to

$$\mathbb{E}[f(\mathbf{x}_t) - f(\mathbf{x}_*)] \leq \frac{G\|\mathbf{x}_0 - \mathbf{x}_*\|}{\sqrt{t+1}}. \tag{13}$$

1182 *Proof.* Since $\|\mathbf{y}_k - \mathbf{x}_*\| \leq \|\mathbf{x}_0 - \mathbf{x}_*\|$ we have that $\mathbb{E}[\|\nabla f(\mathbf{y}_k, \zeta_k)\|^2] \leq G^2$ and re-arranging (48)
 1183 gives

$$\begin{aligned}
 1184 \quad ((t + 1)\mathbb{E}[f(\mathbf{x}_t) - f(\mathbf{x}_*)] + \lambda \sum_{k=0}^t \mathbb{E}[B_f(\mathbf{x}_k, \mathbf{y}_k)])^2_+ &\leq G^2(t + 1)(\|\mathbf{x}_0 - \mathbf{x}_*\|^2 - \|\mathbf{z}_t - \mathbf{x}_*\|^2) \\
 1185 \quad &\leq G^2(t + 1)\|\mathbf{x}_0 - \mathbf{x}_*\|^2.
 \end{aligned}$$

1188 Since the term on the left is always positive we can drop the positive part, taking square roots, and
 1189 dividing through by $t + 1$ gives
 1190

$$1191 \mathbb{E}[f(\mathbf{x}_t) - f(\mathbf{x}_*)] + \frac{\lambda}{t+1} \sum_{k=0}^t \mathbb{E}[B_f(\mathbf{x}_k, \mathbf{y}_k)] \leq \frac{G\|\mathbf{x}_0 - \mathbf{x}_*\|}{\sqrt{t+1}}.$$

1193 Inserting back $\lambda = \beta/(1 - \beta)$ gives
 1194

$$1195 \mathbb{E}[f(\mathbf{x}_t) - f(\mathbf{x}_*)] \leq \mathbb{E}[f(\mathbf{x}_t) - f(\mathbf{x}_*)] + \frac{1}{t+1} \frac{\beta}{1-\beta} \sum_{k=0}^t \mathbb{E}[B_f(\mathbf{x}_k, \mathbf{y}_k)] \leq \frac{G\|\mathbf{x}_0 - \mathbf{x}_*\|}{\sqrt{t+1}}.$$

1198 Finally, we can drop the positive terms given by the Bregman divergences $\mathbb{E}[B_f(\mathbf{x}_k, \mathbf{y}_k)]$, giving
 1199 the final desired result.
 1200 \square
 1201

1202 C PRACTICAL & ADAM VERSIONS OF SCHEDULEP

1204 We can also develop a version of Schedulep that makes use of any preconditioner, such as the
 1205 Adam preconditioner.
 1206

1207 To derive a preconditioned version of Schedulep, let $\mathbf{D}_t \in \mathbb{R}^{d \times d}$ be our positive definite sym-
 1208 metric preconditioner, and let $\|\mathbf{z}\|_{\mathbf{D}_t}^2 := \langle \mathbf{D}_t \mathbf{z}, \mathbf{z} \rangle$ be the norm induced by this preconditioner. The
 1209 preconditioned version of Schedulefree is given by

$$1210 \mathbf{y}_t = (1 - \beta)\mathbf{z}_{t-1} + \beta\mathbf{x}_t \quad (55)$$

$$1212 \mathbf{z}_t = \mathbf{z}_{t-1} - \gamma_t \mathbf{D}_t^{-1} \nabla f(\mathbf{y}_t, \zeta_t) \quad (56)$$

$$1213 \mathbf{x}_{t+1} = (1 - c_{t+1})\mathbf{x}_t + c_{t+1}\mathbf{z}_t \quad (57)$$

1214 We can again upper bound the distance between \mathbf{z}_t and a solution \mathbf{x}_* , but now under the precondi-
 1215 tioned norm via
 1216

$$1217 \|\mathbf{z}_t - \mathbf{x}_*\|_{\mathbf{D}_t}^2 = \|\mathbf{z}_{t-1} - \mathbf{x}_*\|_{\mathbf{D}_t}^2 - 2\gamma_t \langle \mathbf{D}_t^{-1} \nabla f(\mathbf{y}_t, \zeta_t), \mathbf{z}_{t-1} - \mathbf{x}_* \rangle_{\mathbf{D}_t} + \gamma_t^2 \|\nabla f(\mathbf{y}_t, \zeta_t)\|_{\mathbf{D}_t^{-1}}^2 \\ 1218 = \|\mathbf{z}_{t-1} - \mathbf{x}_*\|_{\mathbf{D}_t}^2 - 2\gamma_t \langle \nabla f(\mathbf{y}_t, \zeta_t), \mathbf{z}_{t-1} - \mathbf{x}_* \rangle + \gamma_t^2 \|\nabla f(\mathbf{y}_t, \zeta_t)\|_{\mathbf{D}_t^{-1}}^2. \quad (58)$$

1220 It only remains to bound the linear term $\langle \nabla f(\mathbf{y}_t), \mathbf{z}_{t-1} - \mathbf{x}_* \rangle$ for which we follow the exact same
 1221 steps between (39) and (40) giving

$$1222 \|\mathbf{z}_t - \mathbf{x}_*\|_{\mathbf{D}_t}^2 \leq \|\mathbf{z}_{t-1} - \mathbf{x}_*\|_{\mathbf{D}_t}^2 + \gamma_t^2 \|\nabla f(\mathbf{y}_t, \zeta_t)\|_{\mathbf{D}_t^{-1}}^2 \\ 1223 - 2\gamma_t ((f_{\zeta_t}(\mathbf{y}_t) - f_{\zeta_t}(\mathbf{x}_*)) - 2\beta\gamma_t \langle \nabla f(\mathbf{y}_t, \zeta_t), \mathbf{z}_{t-1} - \mathbf{x}_t \rangle). \quad (59)$$

1224 Minimizing the above in $\gamma_t \geq 0$ gives
 1225

$$1226 \gamma_t = \frac{(f_{\zeta_t}(\mathbf{y}_t) - f_{\zeta_t}(\mathbf{x}_*) + \beta \langle \nabla f(\mathbf{y}_t, \zeta_t), \mathbf{z}_{t-1} - \mathbf{x}_t \rangle)_+}{\|\nabla f(\mathbf{y}_t, \zeta_t)\|_{\mathbf{D}_t^{-1}}^2}. \quad (60)$$

1227 See Algorithm 2 for the complete pseudo-code.
 1228

1229 **Remark C.1** (Practical version). In our code we use a slightly different form given by
 1230

$$1233 \gamma_t = \frac{(f_{\zeta_t}(\mathbf{y}_t) - f_{\zeta_t}(\mathbf{x}_*) + \langle \nabla f(\mathbf{y}_t, \zeta_t), \mathbf{z}_{t-1} - \mathbf{y}_t \rangle)_+}{\|\nabla f(\mathbf{y}_t, \zeta_t)\|^2}. \quad (61)$$

1234 This follows from (41) by using that
 1235

$$1236 \mathbf{x}_t = \frac{1}{\beta} \mathbf{y}_t + \left(1 - \frac{1}{\beta}\right) \mathbf{z}_{t-1}$$

1237 thus
 1238

$$1239 \mathbf{z}_{t-1} - \mathbf{x}_t = \frac{1}{\beta} \mathbf{z}_{t-1} - \frac{1}{\beta} \mathbf{y}_t.$$

Algorithm 2 Adam-Schedulep: Adam Schedule Free Polyak

```

1: Input:  $z_{-1} = \mathbf{x}_0 \in \mathbb{R}^d$ ,  $\beta \in [0, 1]$ ,  $c_t > 0$ 
2: for  $t = 0$  to  $T - 1$  do
3:    $\mathbf{y}_t = (1 - \beta)z_t + \beta \mathbf{x}_t$ 
4:    $\gamma_t = \frac{[f_{\zeta_t}(\mathbf{y}_t) - f_{\zeta_t}(\mathbf{x}_*) + \beta \langle \nabla f(\mathbf{y}_t, \zeta_t), z_t - \mathbf{x}_t \rangle]_+}{\|\nabla f(\mathbf{y}_t, \zeta_t)\|_{D_t}^2}$ 
5:    $z_{t+1} = z_t - \gamma_t D_t^{-1} \nabla f(\mathbf{y}_t, \zeta_t)$ 
6:    $\mathbf{x}_{t+1} = (1 - c_{t+1})\mathbf{x}_t + c_{t+1}z_{t+1}$ 
7: end for
8: Return:  $\mathbf{x}_T$ 

```

1253

1254 Thus finally

$$\beta \langle \nabla f(\mathbf{y}_t, \zeta_t), z_{t-1} - \mathbf{x}_t \rangle = \langle \nabla f(\mathbf{y}_t, \zeta_t), z_{t-1} - \mathbf{y}_t \rangle.$$

1255

1256 **D IMPLICATIONS TO MOMENTUM METHOD**

1257

1260 Since primal averaging is a special case of `schedule-free` when $\beta = 1$, and primal averaging
 1261 itself is equivalent to `momentum`, our convergence theory for the `schedule-free` method includes
 1262 `Momentum` as a special case. For example, the last-iterate convergence result in Corollary 2.3 applies
 1263 to the primal averaging method when $\beta = 1$. This is interesting because of the equivalence between
 1264 the primal averaging and momentum.

1265

1266

Algorithm 3 Momentum

```

1: Input:  $\mathbf{x}_0 \in \mathbb{R}^d$ ,  $\mathbf{m}_{-1} = 0$ ,  $\alpha_t \geq 0$ ,  $\lambda_t \geq 0$ .
2: for  $t = 0$  to  $T - 1$  do
3:    $\mathbf{m}_t = \frac{\lambda_t}{1 + \lambda_t} \mathbf{m}_{t-1} + \frac{1}{1 + \lambda_t} \nabla f(\mathbf{x}_t, \zeta_t)$ 
4:    $\mathbf{x}_{t+1} = \mathbf{x}_t - \alpha_t \mathbf{m}_t$ 
5: end for
6: Return:  $\mathbf{x}_T$ 

```

1273

1274 The equivalence of the momentum method and the primal averaging method is shown in the following
 1275 lemma.

1276

1277

Lemma D.1. If $(\mathbf{x}_t)_{t \in \mathbb{N}}$ is generated by the Momentum Algorithm 3 from parameters (α_t, λ_t) ,
 1278 then it verifies the primal averaging iterates by choosing any parameters (γ_t, c_t) satisfying

$$c_1 \gamma_0 = \frac{\alpha_0}{1 + \lambda_0}, \quad (62)$$

1281

and for $t \geq 1$,

$$\alpha_{t-1} \left(\frac{1}{c_t} - 1 \right) \frac{1 + \lambda_t}{\lambda_t} = \frac{\alpha_t}{c_{t+1}}, \quad \text{and} \quad \gamma_t = \frac{\alpha_{t-1}}{\lambda_t} \left(\frac{1}{c_t} - 1 \right). \quad (63)$$

1285

1286

Proof. For the primal averaging iterate, since $z_{-1} = \mathbf{x}_0$,

1287

1288

$$\begin{aligned} \mathbf{x}_1 &= (1 - c_1)\mathbf{x}_0 + c_1(\mathbf{x}_0 - \gamma_0 \nabla f(\mathbf{x}_0, \zeta_0)) \\ &= \mathbf{x}_0 - c_1 \gamma_0 \nabla f(\mathbf{x}_0, \zeta_0). \end{aligned}$$

1290

1291

For the momentum iterate, since $\mathbf{m}_{-1} = 0$,

1292

1293

$$\mathbf{x}_1 = \mathbf{x}_0 - \frac{\alpha_0}{1 + \lambda_0} \nabla f(\mathbf{x}_0, \zeta_0).$$

1294

1295

Hence, they are equivalent when

$$c_1 \gamma_0 = \frac{\alpha_0}{1 + \lambda_0}.$$

1296 Suppose that the iterates of primal averaging and the momentum iterate are equivalent at $(t - 1)$ -st
 1297 and t -th iteration for some $t \geq 1$. Let us show that their iterates at the $(t + 1)$ -st iteration are the
 1298 same; i.e.,

$$1299 \quad \mathbf{x}_{t+1}^{\text{momentum}} = \mathbf{x}_t - \alpha_t \mathbf{m}_t = (1 - c_{t+1}) \mathbf{x}_t + c_{t+1} \mathbf{z}_t = \mathbf{x}_{t+1}^{\text{PA}},$$

1300 equivalently,

$$1301 \quad \mathbf{z}_t = \mathbf{x}_t - \frac{\alpha_t}{c_{t+1}} \mathbf{m}_t. \quad (64)$$

1303 Indeed, by the induction hypothesis, we have

$$1305 \quad \mathbf{z}_{t-1} = \mathbf{x}_{t-1} - \frac{\alpha_{t-1}}{c_t} \mathbf{m}_{t-1}. \quad (65)$$

1307 By the updating rule of the primal averaging method and (65), we have

$$\begin{aligned} 1308 \quad \mathbf{z}_t &= \mathbf{z}_{t-1} - \gamma_t \nabla f(\mathbf{x}_t, \zeta_t) \\ 1309 &= \mathbf{x}_{t-1} - \frac{\alpha_{t-1}}{c_t} \mathbf{m}_{t-1} - \gamma_t \nabla f(\mathbf{x}_t, \zeta_t) \\ 1310 &= \mathbf{x}_t - \alpha_{t-1} \left(\frac{1}{c_t} - 1 \right) \mathbf{m}_{t-1} - \gamma_t \nabla f(\mathbf{x}_t, \zeta_t) \\ 1311 &= \mathbf{x}_t - \alpha_{t-1} \left(\frac{1}{c_t} - 1 \right) \frac{1 + \lambda_t}{\lambda_t} \mathbf{m}_t - \left(\gamma_t - \frac{\alpha_{t-1}}{\lambda_t} \left(\frac{1}{c_t} - 1 \right) \right) \nabla f(\mathbf{x}_t, \zeta_t). \end{aligned}$$

1316 The last two lines follow from the updating rule of the momentum method. Hence, we have
 1317 shown (64) to hold when

$$1319 \quad \alpha_{t-1} \left(\frac{1}{c_t} - 1 \right) \frac{1 + \lambda_t}{\lambda_t} = \frac{\alpha_t}{c_{t+1}}, \quad \text{and} \quad \gamma_t = \frac{\alpha_{t-1}}{\lambda_t} \left(\frac{1}{c_t} - 1 \right).$$

1321 \square

1323 The above lemma shows that, as long as the hyperparameters for primal averaging and momentum
 1324 method satisfy (62) and (63), we have the momentum method equivalent to the primal averaging
 1325 method.

1326 Since the primal averaging method is a special case of `schedule-free` (when $\beta_t \equiv \beta = 1$),
 1327 the convergence result in Theorem 2.1 gives the convergence for the momentum method whenever
 1328 (α_t, λ_t) in Algorithm 3 satisfies (6), (62), (63). To illustrate this, we start showing the convergence
 1329 of the momentum method when its stepsize $\{\alpha_t\}_{t=0}^T$ is given by some schedule.

1331 **Corollary D.2.** Let $\{\alpha_t\}_{t=0}^T$ be given by some scheduler. Initializing λ_0, γ_0 such that $(1 + \lambda_0)\gamma_0 -$
 1332 $\alpha_0 > 0$, consider $\{\gamma_t\}_{t=0}^{T-1}, \{\lambda_t\}_{t=0}^{T-1}$ such that $\gamma_1 = \frac{\alpha_0\gamma_0}{(1 + \lambda_0)\gamma_0 - \alpha_0} > 0$ and for $t = 1, \dots, T - 1$,

$$1334 \quad \lambda_t = \frac{\alpha_{t-1}}{\gamma_t^2} \sum_{i=0}^{t-1} \gamma_i, \quad \gamma_{t+1} = \frac{\alpha_t \sum_{i=0}^t \gamma_i}{\frac{\alpha_{t-1}}{\gamma_t} \left(\sum_{i=0}^{t-1} \gamma_i \right) + \gamma_t - \alpha_t}. \quad (66)$$

1337 Suppose that

$$1339 \quad \alpha_t < \frac{\alpha_{t-1}}{\gamma_t} \left(\sum_{i=0}^{t-1} \gamma_i \right) + \gamma_t. \quad (67)$$

1341 Then Algorithm 3 with parameters (α_t, λ_t) for $t = 0, 1, \dots, T - 1$ would then give the convergence

$$1343 \quad \mathbb{E}[f(\mathbf{x}_T) - f(\mathbf{x}_*)] \leq \frac{\frac{1}{2} \|\mathbf{x}_0 - \mathbf{x}_*\|^2 + \gamma_0(f(\mathbf{x}_0) - f(\mathbf{x}_*))}{\sum_{t=0}^T \gamma_t} + \sum_{t=0}^T \frac{\frac{1}{2} \gamma_t^2 G^2}{\sum_{t=0}^T \gamma_t}. \quad (68)$$

1346 *Proof.* From (6), we know that

$$1348 \quad \frac{1}{c_t} - 1 = \frac{\sum_{i=0}^t \gamma_i}{\gamma_t} - 1 = \frac{\sum_{i=0}^{t-1} \gamma_i}{\gamma_t}.$$

1350 Hence, putting (6) into (62) and (63), we have that
 1351

$$1352 \frac{\gamma_0 \gamma_1}{\gamma_0 + \gamma_1} = \frac{\alpha_0}{1 + \lambda_0}, \quad (69)$$

$$1354 \alpha_{t-1} \frac{\sum_{i=0}^{t-1} \gamma_i}{\gamma_t} \frac{1 + \lambda_t}{\lambda_t} = \frac{\alpha_t}{\gamma_{t+1}} \sum_{i=0}^{t+1} \gamma_i, \quad (70)$$

$$1357 \gamma_t^2 = \frac{\alpha_{t-1}}{\lambda_t} \left(\sum_{i=0}^{t-1} \gamma_i \right). \quad (71)$$

1360 We see that (69) gives
 1361

$$(1 + \lambda_0) \gamma_0 \gamma_1 = \alpha_0 \gamma_0 + \alpha_0 \gamma_1,$$

1362 which implies
 1363

$$\gamma_1 = \frac{\alpha_0 \gamma_0}{(1 + \lambda_0) \gamma_0 - \alpha_0}.$$

1365 Since $(1 + \lambda_0) \gamma_0 - \alpha_0 > 0$, we have $\gamma_1 > 0$. Consider $t = 1, \dots, T - 1$. Rearranging (71), we can
 1366 easily obtain

$$1367 \lambda_t = \frac{\alpha_{t-1}}{\gamma_t^2} \sum_{i=0}^{t-1} \gamma_i. \quad (72)$$

1370 For (70), we see that
 1371

$$1372 \alpha_{t-1} \frac{\sum_{i=0}^{t-1} \gamma_i}{\gamma_t} \frac{1 + \lambda_t}{\lambda_t} = \frac{\alpha_t}{\gamma_{t+1}} \sum_{i=0}^{t+1} \gamma_i = \frac{\alpha_t}{\gamma_{t+1}} \left(\sum_{i=0}^t \gamma_i \right) + \alpha_t. \quad (73)$$

1374 Since (72) implies
 1375

$$\frac{1 + \lambda_t}{\lambda_t} = \frac{1}{\lambda_t} + 1 = \frac{\gamma_t^2}{\alpha_{t-1} \left(\sum_{i=0}^{t-1} \gamma_i \right)} + 1, \quad (74)$$

1378 (73) then gives
 1379

$$1380 \gamma_t + \alpha_{t-1} \frac{\sum_{i=0}^{t-1} \gamma_i}{\gamma_t} - \alpha_t = \frac{\alpha_t}{\gamma_{t+1}} \left(\sum_{i=0}^t \gamma_i \right),$$

1383 and hence,

$$1384 \gamma_{t+1} = \frac{\alpha_t \left(\sum_{i=0}^t \gamma_i \right)}{\alpha_{t-1} \frac{\sum_{i=0}^{t-1} \gamma_i}{\gamma_t} + \gamma_t - \alpha_t}.$$

1388 This is positive when
 1389

$$1390 \alpha_t < \alpha_{t-1} \frac{\sum_{i=0}^{t-1} \gamma_i}{\gamma_t} + \gamma_t.$$

1392 \square

1394 Given the stepsize α_t of the momentum method, the lemma suggests the choice of the momentum
 1395 parameter $\{\lambda_t\}_{t=0}^{T-1}$ such that the last-iterate convergence theory holds. The stepsize $\{\alpha_t\}_{t=0}^T$ then
 1396 defines a set of parameters $\{\gamma_t\}_{t=0}^T$, which determines the convergence rate of momentum as shown
 1397 in (68).
 1398

1399 On the other hand, if we set the stepsize $\{\gamma_t\}_{t=0}^T$ of the primal averaging following some schedule,
 1400 we can have a new set of hyperparameters for the momentum method that guarantees the theoretical
 1401 convergence.
 1402

1403

1404
 1405 **Corollary D.3.** Let $\{\gamma_t\}_{t=0}^T$ be given by some scheduler. Initializing $\lambda_0 \geq 0$ and $\alpha_0 = \frac{\gamma_0 \gamma_1 (1 + \lambda_0)}{\gamma_0 + \gamma_1}$, consider the iterates generated by the momentum algorithm (Algorithm 3) with parameters (α_t, λ_t) given by
 1406
 1407
 1408

$$\lambda_t = \alpha_{t-1} \frac{\sum_{i=0}^{t-1} \gamma_i}{\gamma_t^2}, \quad \alpha_t = \alpha_{t-1} \frac{\gamma_{t+1}}{\gamma_t} \frac{\sum_{i=0}^{t-1} \gamma_i}{\sum_{i=0}^{t+1} \gamma_i} + \frac{\gamma_t \gamma_{t+1}}{\sum_{i=0}^{t+1} \gamma_i}. \quad (75)$$

1409
 1410 for $t = 1, \dots, T$. We then have the convergence
 1411
 1412

$$\mathbb{E}[f(\mathbf{x}_T) - f(\mathbf{x}_*)] \leq \frac{\frac{1}{2} \|\mathbf{x}_0 - \mathbf{x}_*\|^2 + \gamma_0 (f(\mathbf{x}_0) - f(\mathbf{x}_*))}{\sum_{t=0}^T \gamma_t} + \sum_{t=0}^T \frac{\frac{1}{2} \gamma_t^2 G^2}{\sum_{t=0}^T \gamma_t}. \quad (76)$$

1413
 1414 Let $D := \|\mathbf{x}_0 - \mathbf{x}_*\|$. In particular for the constant learning rate $\gamma_t \equiv \gamma = \frac{D}{G\sqrt{T}}$ gives the rate
 1415
 1416

$$\mathbb{E}[f(\mathbf{x}_T) - f(\mathbf{x}_*)] \leq \frac{f(\mathbf{x}_0) - f(\mathbf{x}_*)}{T} + \frac{DG}{\sqrt{T}}. \quad (77)$$

1417
 1418 *Proof.* Putting (6) into (62) and (63), we have (69), (70) and (71) hold. Simply by rearranging terms,
 1419 we obtain
 1420

$$\alpha_0 = \frac{\gamma_0 \gamma_1 (1 + \lambda_0)}{\gamma_0 + \gamma_1}, \quad (78)$$

1421 and for $t = 1, \dots, T-1$,
 1422
 1423

$$\lambda_t = \alpha_{t-1} \frac{\sum_{i=0}^{t-1} \gamma_i}{\gamma_t^2}, \quad \alpha_t = \alpha_{t-1} \frac{\gamma_{t+1}}{\gamma_t} \frac{\sum_{i=0}^{t-1} \gamma_i}{\sum_{i=0}^{t+1} \gamma_i} \frac{1 + \lambda_t}{\lambda_t}.$$

1424 Applying (74), we can simplify this as
 1425
 1426

$$\lambda_t = \alpha_{t-1} \frac{\sum_{i=0}^{t-1} \gamma_i}{\gamma_t^2}, \quad \alpha_t = \alpha_{t-1} \frac{\gamma_{t+1}}{\gamma_t} \frac{\sum_{i=0}^{t-1} \gamma_i}{\sum_{i=0}^{t+1} \gamma_i} + \frac{\gamma_t \gamma_{t+1}}{\sum_{i=0}^{t+1} \gamma_i}.$$

1427 \square

1428
 1429 Similarly, if we have $\{\gamma_t\}_{t=0}^T$ given by some schedule, we can derive the stepsize α_t and the momentum parameter λ_t for momentum and obtain the convergence bound. Moreover, if $\gamma_t \equiv \gamma = \frac{D}{G\sqrt{T}}$, we can obtain the optimal convergence $\mathcal{O}(\frac{D}{G\sqrt{T}})$ for momentum.
 1430
 1431

1432 E EXPERIMENTS: SUPPLEMENTARY MATERIAL

1433 E.1 IMAGE CLASSIFICATION

1434 We conduct experiments on multiple vision models trained on CIFAR10 and CIFAR100, covering both small-scale (ResNet-20) and larger-scale architectures (Wide ResNet (16-8),
 1435 DenseNet). Full details of the architectures and training configurations are provided in Table 1. All
 1436 experiments are based on the open-source framework <https://github.com/fabian-sp/step-back>, which we extend to include the Schedule-free optimizer and to support Group-
 1437 Norm normalization layers rather than BatchNorm for the ResNet⁸ and DenseNet⁹ architectures.
 1438 As mentioned in Section 4, this is to avoid the complication of writing custom BatchNorm
 1439 code to approximate batch statistics of the \mathbf{x} sequence of Schedule-free.
 1440

1441 E.1.1 PREDICTIVE POWER FOR DEEP LEARNING

1442 We train a small ResNet-20 model on CIFAR10 and compute the theoretical bound in Theorem 2.1. The norm of stochastic gradients is used as a proxy for the Lipschitz constant G , while the
 1443

⁸https://github.com/akamaster/pytorch_resnet_cifar10/blob/master/resnet.py

⁹<https://github.com/weiaicunzai/pytorch-cifar100/blob/master/models/densenet.py>

1458

1459

1460

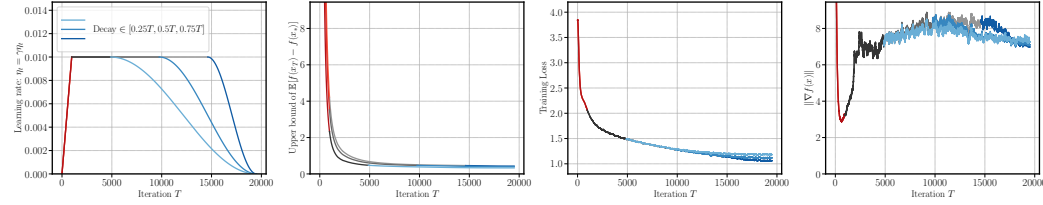
1461

1462

1463

1464

1465

(a) Cosine schedule with base learning rate $\gamma = 0.01$

1466

1467

1468

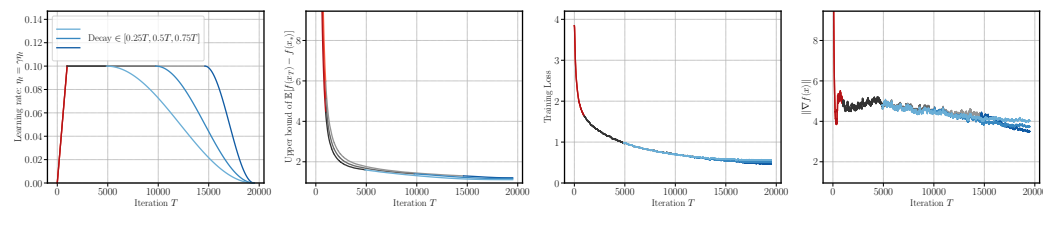
1469

1470

1471

1472

1473

(b) Cosine schedule with base learning rate $\gamma = 0.1$

1474

1475

1476

1477

1478

1479

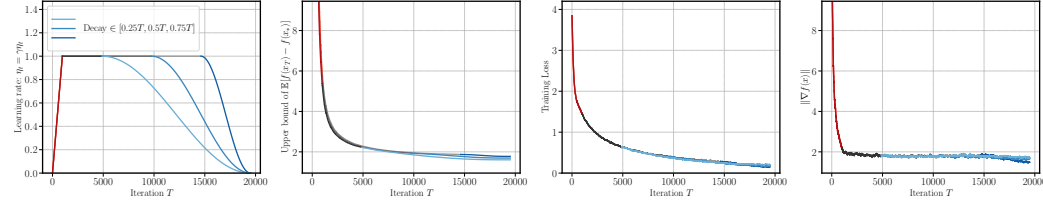
1480

1481

1482

1483

1484

(c) Cosine schedule with base learning rate $\gamma = 1$

1485

1486

1487

1488

1489

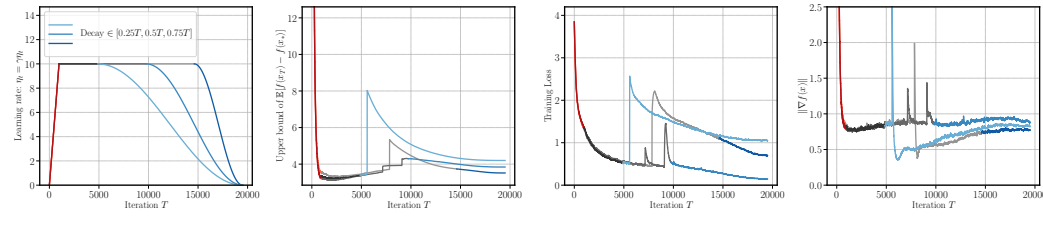
1490

1491

1492

1493

1494

(d) Cosine schedule with base learning rate $\gamma = 10$

1503

1504

Figure 9: Comparison between the convex theory and the training loss for cosine schedule with different cooldown periods and different base learning rates.

1505

1506

1507

1508

1509

1510

1511

Experiment	CIFAR10	CIFAR100
Architectures	ResNet-20 Wide ResNet (16-8)	DenseNet
Normalization Layer	Group Norm	Group Norm
Epochs	50	100
GPUs	1 × A100	1 × A100
Batch size	128	64
Base Learning Rates	[0.01, 0.1, 1, 10]	[0.01, 0.1, 1, 10]
Weight Decay	0.0001	0.0002
Momentum	0.9	0.9
Warm-up fraction	0.05	0.05
Cooldown fraction	0.25	0.05

Table 1: Comparison of architecture and training setup for image classification on CIFAR10 and CIFAR100.

best parameters and loss during training are used to approximate x_* and $f(x_*)$, respectively. We compare our bound for the `wsd` and `cosine` schedules with different cooldown lengths where the decay period begins at iteration $\{0.25T, 0.5T, 0.75T\}$ and T is the training horizon. Figure 3 shows the results for the `wsd` schedule with the base learning rate $\gamma \in \{0.01, 10\}$ and Figure 9 shows the results for the `cosine` schedule with the base learning rate $\gamma \in \{0.01, 0.1, 1, 10\}$. Figure 4 shows the performance of a constant-then-diverging schedule with the base learning rate $\gamma = 10$ and varying diverging lengths.

Since we have discussed Figures 3 and 4 earlier in the paper, we will focus on the discussion over Figure 9 here. In fact, it turns out that both the `wsd` and `cosine` schedules exhibit similar theoretical and empirical performance, so our discussion on the `cosine` schedule is also applicable to `wsd` schedule.

When the base learning rate γ is small (i.e., $\gamma \in \{0.01, 0.1, 1\}$), the theory predicts the convergence of the cosine schedule well. A slight mismatch is that, earlier cooldown gives a slower empirical convergence, while the theory behaves in the opposite way. We also see that the gradient norm is more stable as γ increases. When γ is large (i.e., $\gamma = 10$), the theory successfully predicts the spikes in the training loss for different schedules, regardless of whether the spike occurs *before* or *after* the cooldown begins. One possible explanation is that, the spikes in the gradient norms (which is used to approximate the Lipschitz constant G in the theory) lead to the spikes in the theoretical bound. Yet, one should also note that, when $\gamma = 0.01$, the blowup in the gradient norm does not lead to the divergence in the theoretical bound, and both the theoretical bound and the training loss converge.

E.1.2 STABILITY ANALYSIS

We compare the stability and the performance of Schedule-free variants and SGD-m. We evaluate both training dynamics and generalization. Models follow the setup in Defazio et al. (2024) for some of the tasks in AlgoPerf: a Wide ResNet (16-8) trained on CIFAR10 (a smaller model) and a DenseNet trained on CIFAR100 (a larger model). Hyperparameters and the setting details are listed in Table 1. We use wsd schedule for SGD-m, schedulet and Schedule-free with $c_t = 1/t$ from previous theory, and use wamrup-stable schedule only for Schedule-free with the heuristic parameters $c_t = \gamma_t^2 / \sum_{i=1}^t \gamma_i^2$.

Figure 6 shows the training performance (in terms of the training loss and the validation score) against the learning rate or the number of epochs when training a Wide ResNet (16-8) model on the CIFAR10 data set. We see that, when the learning rate is small, SGD- m has a better performance over schedule-free, both in terms of the training loss and the validation score. When the learning rate is large, SGD- m becomes unstable and Schedule-free outperforms SGD- m . However, we see that schedule-free has a more stable performance in generalization across different learning rates, regardless of the choice of the averaging parameter. In general, schedule has a similar generalization performance as Schedule-free with the heuristic averaging parameter c_t .

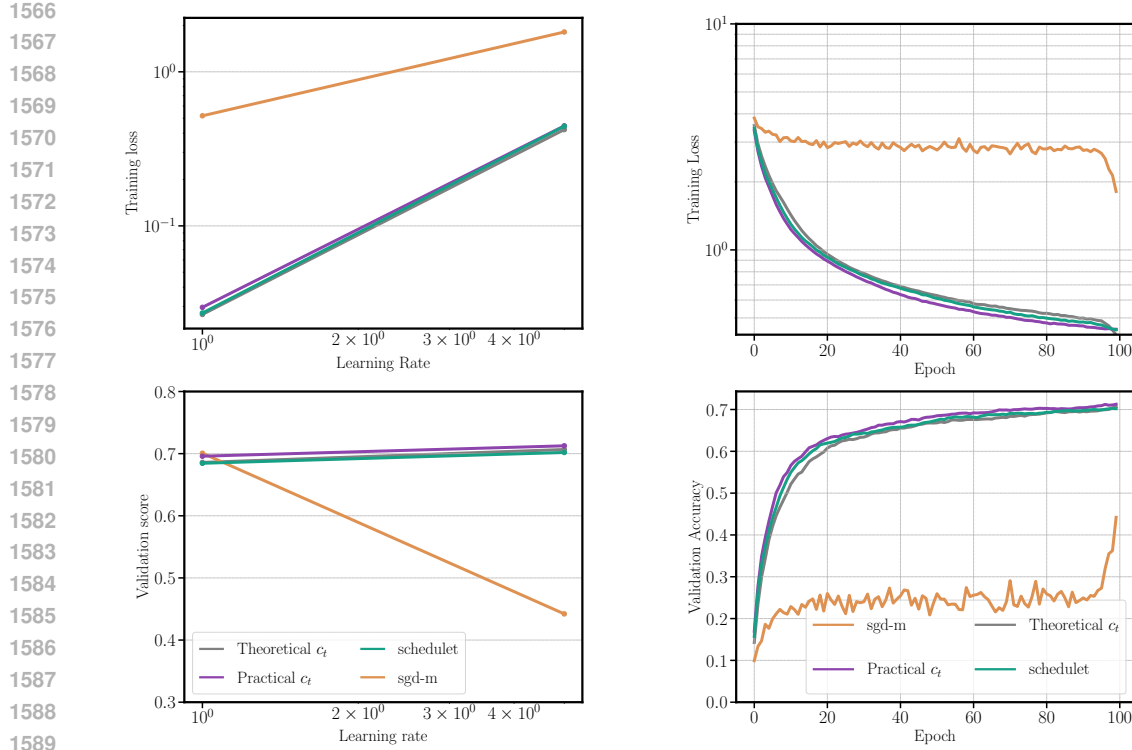


Figure 10: Training a DenseNet model on the CIFAR100 data set.

Figure 10 shows the training performance when training a DenseNet model on the CIFAR100 data set. In this case, Schedule-free performs remarkably better than SGD-m and is robust over different learning rates. Different choices of averaging parameter c_t have similar performance across different learning rates.

E.2 BLACK-BOX DISTILLATION DETAILS

Mixed precision training was enabled using `bfloat16` for efficiency. The student model utilized flash attention (Dao et al., 2022).

Experiment	<code>tiny_shakespeare</code>	<code>fineweb1B</code>
Teacher model	<code>gpt2-medium</code>	EleutherAI/ <code>gpt-j-6B</code>
Student hidden size	768	768
Student transformer layers	4	12
Student attention heads	8	12
Student vocabulary size	50257	50257
Batch size	4	32
Context length	512 tokens	1024 tokens
Tokens per training step	4096	262144
Learning rate schedule	Warm-up \rightarrow Constant \rightarrow Linear	Warm-up \rightarrow Constant \rightarrow Linear
Warm-up fraction	0.1	0.1
Cooldown fraction	—	0.1

Table 2: Comparison of model configurations and training setups for distillation on `tiny_shakespeare` and `fineweb1B`.